

# 1 Probabilistic Seismic Hazard Assessment for a 2 New-build Nuclear Power Plant Site in the UK

3 **Iain J. Tromans<sup>a</sup>, Guillermo Aldama-Bustos<sup>a</sup>, John Douglas<sup>b</sup>, Angeliki**  
4 **Lessi-Cheimariou<sup>a</sup>, Simon Hunt<sup>c</sup>, Manuela Davi<sup>a</sup>, Roger M. W. Musson<sup>d</sup>,**  
5 **Graham Garrard<sup>c</sup>, Fleur O. Strasser<sup>e</sup>, Colin Robertson<sup>f</sup>**

6 A probabilistic seismic hazard analysis (PSHA) has been conducted as part of  
7 the Safety Case justification for a new-build nuclear power plant in the UK. The  
8 study followed a cost-efficient methodology developed by CH2M and associates  
9 for safety-significant infrastructure where high-level regulatory assurance is  
10 required. Historical seismicity was re-evaluated from original sources. The  
11 seismicity model considered fourteen seismic sources which, when combined,  
12 formed six alternative seismic source models. Separate models for the median  
13 ground-motion and aleatory variability were considered. The median ground-  
14 motion model comprised a suite of ground-motion equations adjusted to the site-  
15 specific conditions using  $V_S$ -kappa factors. A partially non-ergodic sigma model  
16 was adopted with separate components for the inter-event variability, and single-  
17 station intra-event variability, adjusted by a partially ergodic site-to-site variability  
18 term. Site response analysis was performed using equivalent-linear random  
19 vibration theory with explicit incorporation of the variability in the ground  
20 properties using Monte Carlo simulations. The final PSHA results were obtained  
21 by convolution of the hazard at the reference rock horizon with the site  
22 amplification factors. The overall epistemic uncertainty captured by the logic tree  
23 was assessed and compared against results from earlier PSHA studies for the same  
24 site.

25 *Keywords: PSHA, Nuclear Power Plants, Seismic Hazard, Hinkley Point, UK*

---

Corresponding author:

Guillermo Aldama-Bustos; [Guillermo.Aldama-Bustos@jacobs.com](mailto:Guillermo.Aldama-Bustos@jacobs.com); +44 (0) 20 3479 8417

<sup>a</sup> Jacobs, Elms House, 43 Brook Green, W6 7EF, London, U.K.

<sup>b</sup> University of Strathclyde, James Weir Building, 75 Montrose Street, G1 1XJ, Glasgow, U.K.

<sup>c</sup> Jacobs, Burderop Park, SN4 0QD, Swindon, U.K.

<sup>d</sup> University of Edinburgh, School of Geosciences, James Hutton Road, EH3 3FE, Edinburgh, U.K.

<sup>e</sup> Independent consultant / Jacobs, Elms House, 43 Brook Green, W6 7EF, London, U.K.

<sup>f</sup> NNB GenCo, Bridgewater House, Counterslip, BS1 6BX, Bristol, U.K.

26 **1. Introduction**

27 Ageing energy infrastructure along with requirements for reliable, low-carbon electricity  
28 has led the UK government to plan a new fleet of nuclear power plants (NPPs) (BERR 2007).  
29 The first of these NPPs to be constructed is Hinkley Point C (HPC), in Somerset, South West  
30 England, which is being developed by NNB GenCo, a subsidiary of EDF Energy. HPC will  
31 be the first NPP to be built in the UK for over 25 years and will consist of a twin UK  
32 European Pressurized Reactor (EPR) which is expected to provide 7% of the UK’s electricity  
33 needs once completed.

34 In March 2014, NNB GenCo appointed CH2M (now Jacobs) to carry out a site-specific  
35 PSHA for the HPC site. In order to meet UK regulatory requirements and provide long-term  
36 support to the safety case, the utility operator (NNB GenCo) requires a probabilistic seismic  
37 hazard assessment (PSHA) to be undertaken for the site under consideration. The PSHA must  
38 include a robust assessment of the earthquake-related hazards to modern standards, and to the  
39 satisfaction of the Office for Nuclear Regulation (ONR).

40 However, given the ONR’s non-prescriptive regulatory approach and that the last seismic  
41 safety case for a NPP presented to the UK regulator was over 25 years ago, there was a lack  
42 of detailed guidance as to the level of sophistication of the PSHA needed to satisfy the  
43 ONR’s regulatory requirements for the new generation of NPPs.

44 Based on experience with the UK regulatory environment, through decades of  
45 involvement in nuclear-related projects, and on the understanding of international best  
46 practice for the evaluation of the seismic hazard for nuclear facilities, core members of the  
47 project delivery team developed a cost-efficient methodology for the PSHA, presented in the  
48 companion paper by Aldama-Bustos et al. (2018). The proposed methodology incorporated  
49 “relevant good practice”, likely to satisfy ONR’s requirements, whilst acknowledging  
50 commercial and program constraints associated with the development of NPPs faced by  
51 utility operators in the UK. The current paper focuses more specifically on the technical  
52 aspects of the PSHA undertaken for the HPC site. The results of this study underpinned the  
53 HPC design basis spectrum and provided inputs to inform the probabilistic safety assessment  
54 for the Safety Case.

55 **2. Gap Analysis and Data Collection**

56 The initial stage of the HPC study consisted of a high-level review of previous studies  
57 and existing data relevant to the site with the objective of identifying data gaps and

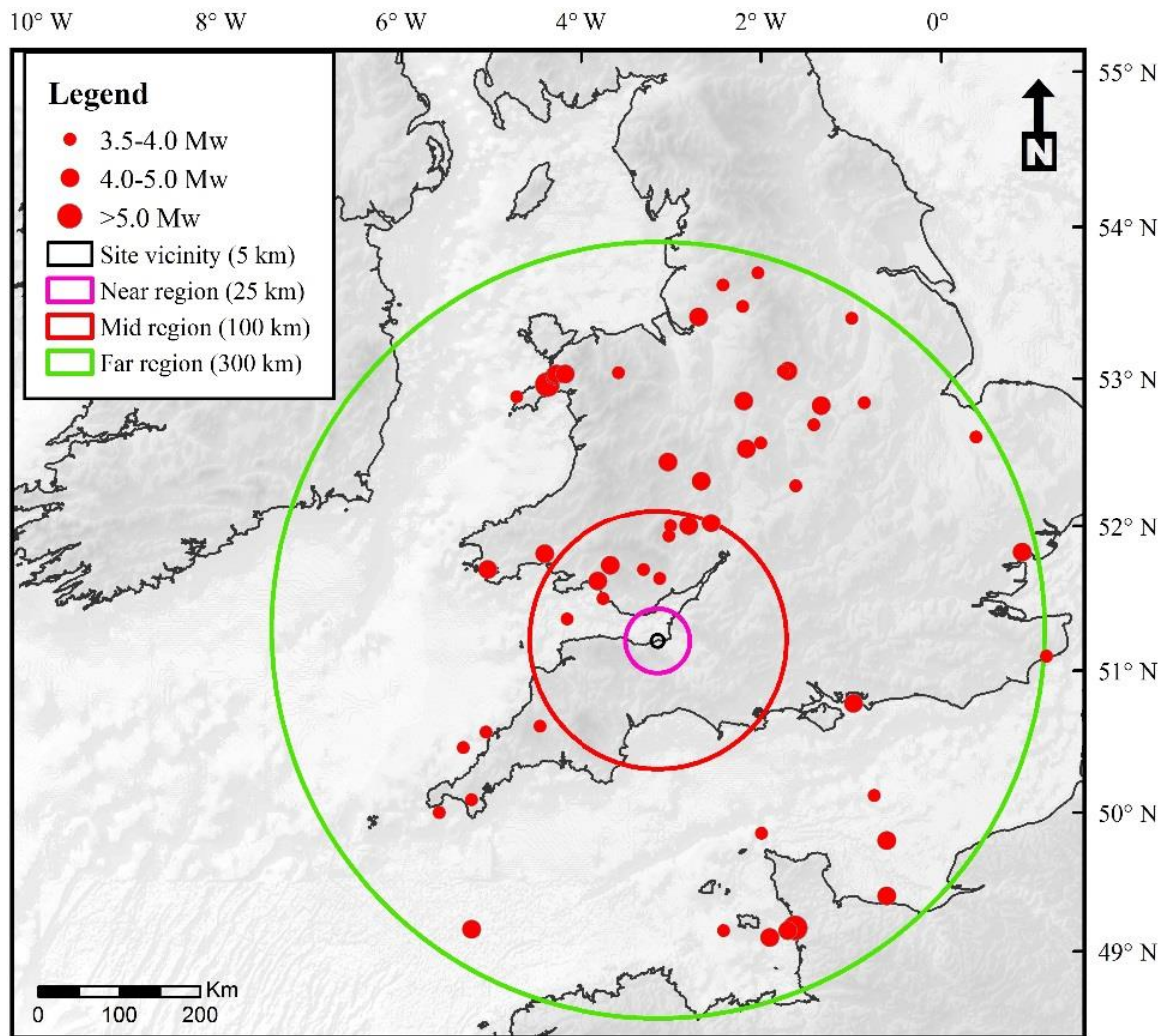
58 streamlining the proposed PSHA methodology. This gap analysis was followed by a more  
59 detailed assessment of the available data and collation of additional data, mainly regarding  
60 the earthquake catalogue, instrumental and macroseismic ground-motion data and ambient-  
61 noise measurements, with the aim of informing the development of the Seismicity Model and  
62 Ground Motion Model. Key findings from this phase are summarized below.

### 63 **2.1. Geology and Tectonics**

64 The data-review efforts focused on four spatial areas colloquially referred to as the ‘study  
65 areas’ (Figure 1). These were adapted from the International Atomic Energy Agency (IAEA)  
66 guidelines SSG-9 (IAEA 2010) which recognize four review extents (from local to regional):  
67 Site Area, Site Vicinity, Near Region and Region. For this study, the IAEA ‘Region’ was  
68 sub-divided into a Mid Region (<100 km) and Far Region (<300 km), to achieve a more  
69 gradational coverage towards the limit of the study area, to help assess major structural  
70 features and to be consistent with the approach adopted for the development of the  
71 earthquake catalogue.

72 The review focused on the tectonic evolution of the Far Region (principal stress  
73 directions, relative crustal movements) and geological evolution and neotectonic  
74 characteristics of the Mid Region (evidence of faulting and seismicity). New data sources  
75 within 100 km of the site were identified and reviewed to ascertain if any could be used to  
76 validate the published interpretations. No investigations providing data on the basement  
77 geology (deep boreholes or seismic reflection profiles) had been undertaken in the last 25  
78 years. Consideration was given to acquiring and reprocessing existing geophysical and  
79 neotectonic datasets, but this was discounted on the basis that reprocessing would not  
80 significantly improve the resolution to an extent that would enable markedly different  
81 interpretations to be made. In addition, given the limited time for the current study, the  
82 assessment was reliant on existing published interpretations.

83 The review identified major geological structures and regions having similar crustal  
84 composition, and the confidence levels that could be placed on such interpretations, to assist  
85 the subsequent development of the seismic source model.



86

87 **Fig. 1** Earthquakes within 300 km of Hinkley Point with  $M \geq 3.5$  since 1850, and study review  
 88 extends (i.e., Site Area, Site Vicinity, Near Region, Mid Region and Far Region)

89 **2.2. Earthquake Catalogue**

90 A project-specific earthquake catalogue was developed. This comprised all events (and  
 91 associated parameters) from the BGS earthquake database that occurred within 300 km of the  
 92 site since 1970, the start of modern instrumental seismic monitoring in the UK. Historical  
 93 events (those prior to 1970) within 100 km of the site were reassessed as part of the current  
 94 study. Other relevant available publications (i.e., Principia Mechanica Ltd. 1982; Soil  
 95 Mechanics Ltd. 1982; Burton et al. 1984; SHWP 1987; Musson 1989, 1994, 2008) were also  
 96 reviewed to ensure completeness of the catalogue.

97 A comprehensive archive search was undertaken to collect data on known events and to  
 98 identify previously undiscovered earthquakes. The search documented 120 events within 100  
 99 km of HPC between 1000 and 1969. A total of 72 earthquakes were reassessed from original

100 data. Of these, 27 do not appear in existing catalogues, and 25 of these were previously  
101 unknown, although most of these proved to be mining-related events.

102 The parameters for reassessed events were derived using the methods outlined in Musson  
103 (1996) and Musson et al. (2001). The BGS database does not generally contain parameters  
104 for earthquakes before 1700, except for a few large and well-documented events. For this  
105 study, and where data existed, an effort was made to obtain at least approximate source  
106 parameters for these earthquakes. New parameters were not assigned for events before 1600  
107 occurring more than 100 km from the site.

108 The parameters for post-1970 events were taken directly from the BGS earthquake  
109 catalogue. This lists 393 events within 100 km of Hinkley Point between 1 January 1970 and  
110 31 July 2014. Of these, seven are larger than  $M$  3 (where  $M$  is the moment magnitude), one  
111 being a foreshock. Magnitudes expressed as  $M_L$  were converted to  $M$  using a well-  
112 constrained formula taken from Grünthal et al. (2009).  $M_L$ - $M$  relationships derived using UK  
113 data were explored (Musson 2005; Edwards et al. 2008; Sargeant and Ottemöller 2009);  
114 however, these were disregarded as they are constrained only for small magnitudes ( $M < 5$ )  
115 using a relatively limited database. Uncertainty in magnitudes, both as a result of inherent  
116 uncertainty and conversion, was not taken into account, as has been the practice in UK PSHA  
117 in the past. It is shown in Musson (2012) that this complex issue is not easily dealt with.

118 The final earthquake catalogue used for the study contains 155 earthquakes (prior to  
119 declustering). Figure 1 shows only those events in the catalogue with  $M \geq 3.5$  since 1850,  
120 providing a reflection of the spatial pattern of seismicity. What emerges is that the seismicity  
121 of the study area is neither uniform nor random. The distribution is dominated by a band of  
122 seismicity running SW-NE from South Wales up to the East Midlands, while a cluster of  
123 earthquake activity occurs in North-Western Wales. Elsewhere there is a scattering of  
124 activity, but with a general scarcity of events in the south and east of England (Whittaker et  
125 al. 1989; Chadwick et al. 1996, Musson 2007).

### 126 **2.3. Ground Motion Data Collation**

127 Ground-motion data relevant to the HPC site was collected and reviewed at an early stage  
128 of the study. These data included instrumental and macroseismic ground-motion data from  
129 permanent networks and historical documentation as well as recordings from a temporary  
130 microseismic network installed and operated by the Seismic Hazard Working Party (SHWP)  
131 between 1985 and the early 1990s.

### 2.3.1. Instrumental and Macroseismic Data

The main objective of the collation, review and assessment of instrumental and macroseismic data was to inform the assessment and final selection of the suite of GMPEs to be considered in the site-specific ground-motion model (GMM) for HPC. With this objective in mind, selection criteria were defined to identify suitable events, from which useful data might be available, as follows:

- From 1970 to the present for UK events, and from 1962 (the date of the establishment of the CEA LDG network) for events in northern France reported in the SI-Hex earthquake catalogue (Francesseisme 2014; Cara et al. 2015). This criterion was established to include only events with good quality data and with reliable magnitude estimates.
- Events with epicentral locations within 600 km of HPC and within the stable continental region as defined by Delavaud et al. (2012). This limited the selection to events occurring in the same tectonic region as Hinkley Point.
- Events with moment magnitude  $M \geq 4.0$  which is the lower magnitude limit covered by most of the modern GMPEs considered likely to be included in the HPC GMM [Note: An initial search was carried out using the criterion  $M_L > 4.0$  (where  $M_L$  is local magnitude) which resulted in some events with magnitude slightly below  $M$  4.0 being included in the final database].
- Events with macroseismic data for at least three different intensity levels to exclude events with insufficient number of intensity observations to demonstrate the attenuation of the ground motion with distance. Events with instrumental but no macroseismic data were retained.

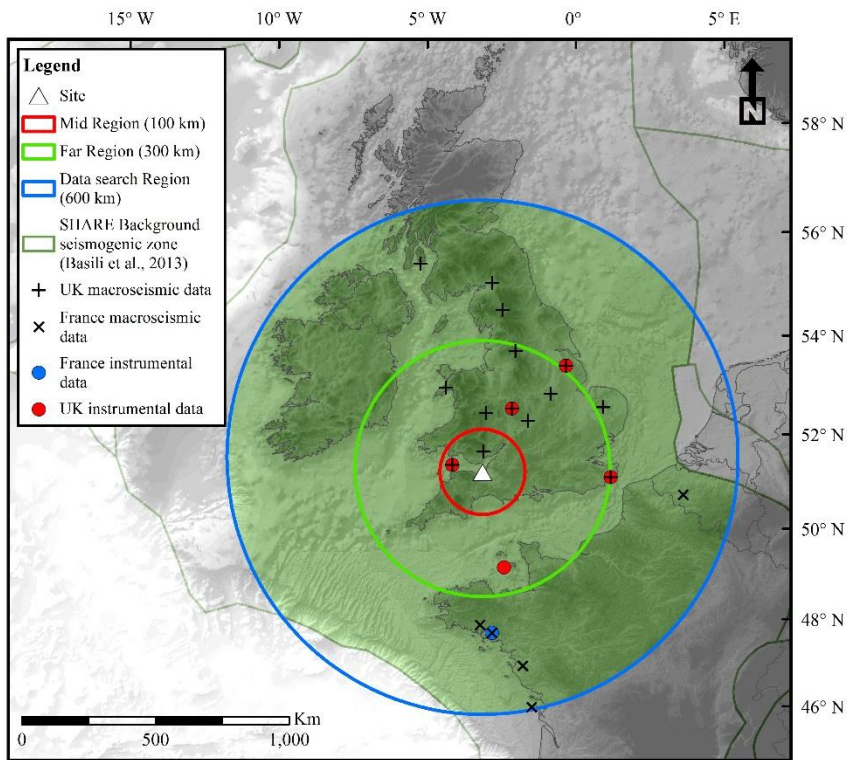
Using the above criteria, a total of 21 events were initially identified from the data sources. Following the pre-processing of the macroseismic raw data, the final data set comprised: 19 events with macroseismic data, and six events with instrumental data, five of which also included macroseismic data. A map showing the epicentral locations of all events in the final dataset is presented in Figure 2.

### 2.3.2. SHWP Microseismic Network

A site-specific seismic hazard study for Hinkley Point A power station, adjacent to the proposed location for HPC, was carried out in the late 1980s by the Seismic Hazard Working Party (SHWP 1987, 1989). A temporary microseismic network was established as part of the

163 SHWP investigation which began in the 1980s (SHWP 1987). The network, which operated  
164 from May 1985, comprised seven stations within a 40-km radius of Hinkley Point and  
165 included a station at the existing NPP.

166 Relevant data associated with events recorded between 1985 and 1994 were made  
167 available by Dr Willy Aspinall, an original SHWP member who set up and ran the network.  
168 These data comprised a total of 368 velocity time-histories from 26 earthquakes, with  
169 magnitudes ranging between 1.0 and 5.1  $M_L$ , and two underwater explosions. Of these  
170 records, only 143 were considered usable, with a signal-to-noise ratio higher than 3 within the  
171 frequency range of interest for the derivation of  $\kappa$ , which in this case was defined as 10-20  
172 Hz. These 143 records were then used in an attempt to obtain an estimate of site-specific  $\kappa$  for  
173 the Hinkley PSHA as described in Section 4.1.2.



174  
175 **Fig. 2** Map of epicentral locations for events with macroseismic and / or instrumental data available.  
176 Base map shows the tectonic regions as defined for the SHARP project (Delavaud et al. 2012, Basili  
177 et al. 2013). The green shaded region indicates the stable continental region within the 600-km radius

## 178 2.4. Site Characterization

179 The initial site characterization gap analysis and data evaluation involved review of  
180 information from ground investigations spanning close to five decades, which included  
181 almost 300 boreholes drilled within the area of the Hinkley Point C site, of which more than  
182 30 were deeper than 100 m. This information, together with data from several rounds of

183 geophysical investigations, were used by the client to create a comprehensive geological  
184 model of the site, which was available for use in this study. Following completion of the gap  
185 analysis, it was considered beneficial to undertake additional non-intrusive field  
186 investigations at the HPC site to improve the understanding of the site response. Two phases  
187 of microtremor surveys, based on ambient noise vibration, were carried out. The Phase 1  
188 survey involved single-station ambient noise measurements at four distinct locations across  
189 the site, while the Phase 2 survey extended the spatial coverage across a wider range of  
190 geological conditions to help in the interpretation of the Phase 1 results. Both surveys were  
191 undertaken by BRGM and followed the well-established SESAME guidelines (Bard et al.  
192 2004; Bard 2008).

### 193 **3. Seismicity Model**

194 The UK lies within an intraplate area with low to moderate levels of seismicity and no  
195 distinct seismogenic structures. In this setting, the seismicity model development was  
196 subdivided into the following phases:

- 197 • Seismic source zonation: Define areas with similar tectonic and geological characteristics  
198 within which one may expect broadly consistent levels of seismicity (i.e., recurrence rates  
199 and magnitude distribution of future earthquake can be reasonably expected to be  
200 uniform).
- 201 • Seismogenic fault identification: Determine if any faults within the defined sources zones  
202 localize seismicity above the background levels for the zone.
- 203 • Seismic source model (SSM) development: Develop SSM logic tree to account for  
204 alternative interpretations of zone boundaries and activity rates, and assign weights to  
205 each alternative branch.

206 The development approach is deemed to be consistent with the principles for source  
207 model development suggested in IAEA SSG-9.

#### 208 **3.1. Definition of Alternative SSMs**

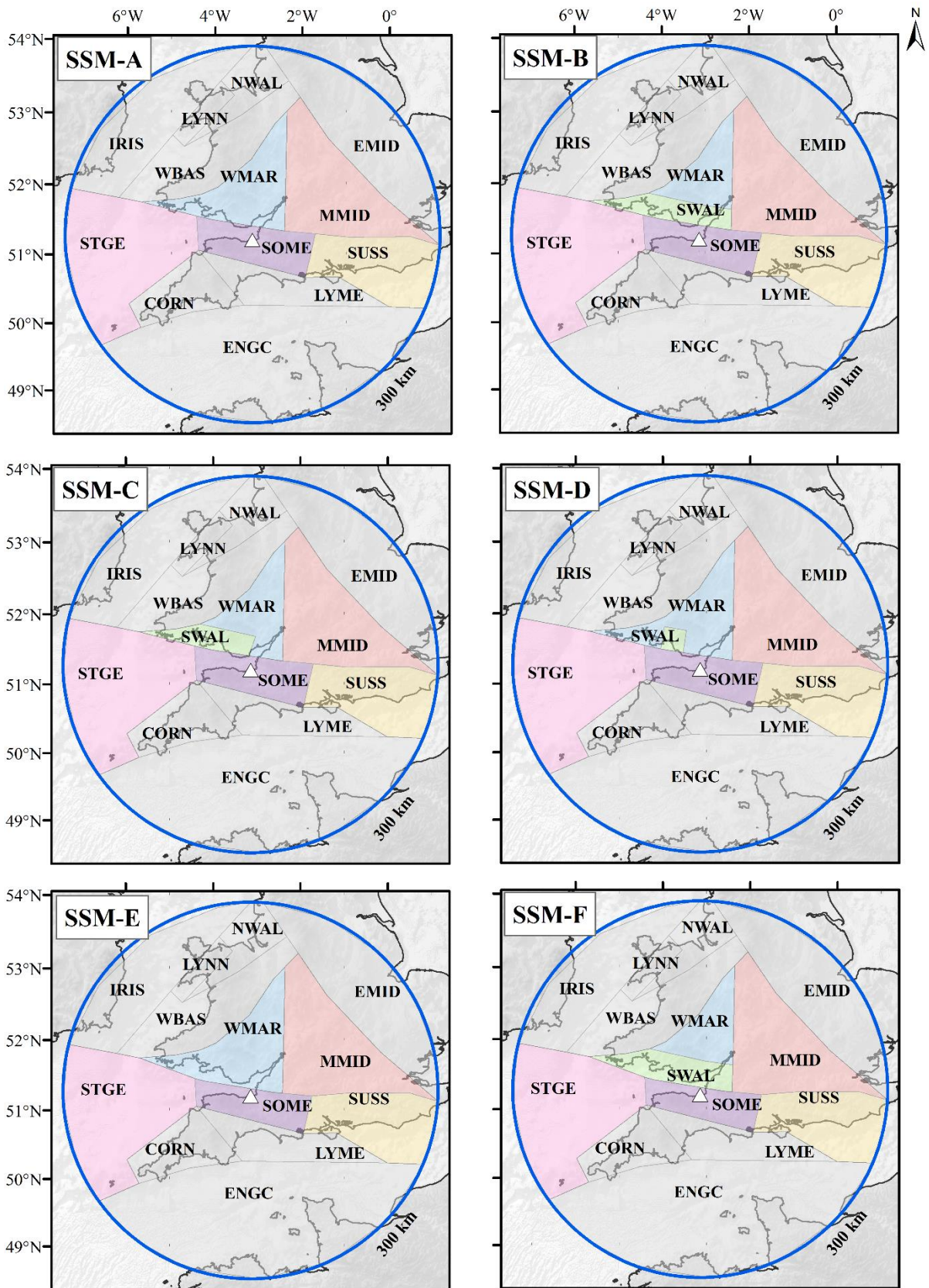
209 The development of alternative SSMs focused mainly on the Mid Region (see Figure 1)  
210 and in particular the variation in seismicity north of the Bristol Channel. Definition of the  
211 source zone boundaries and associated uncertainty used both geological and seismological  
212 evidence and hypotheses, coupled with the spatial variation of the earthquake catalogue  
213 completeness.

214 The main source of uncertainty in the seismicity model was the position of the boundary  
215 between the higher levels of seismicity in South Wales and the lower levels observed south of  
216 the Bristol Channel. This boundary was linked to the Variscan Front, a vague term for the  
217 linear region which runs east-west along the northern part of the Bristol Channel, and that  
218 defines the northern limit of Variscide-type deformation. To the south occurs a zone of  
219 shallow, southerly dipping, broadly east-west trending Variscan thrust, and NW-SE trending  
220 strike-slip faults (i.e., SOME seismic source in Figure 3). To the north is the Wrekin Terrane,  
221 an area of meta-sedimentary and plutonic basement rocks overlain by volcano-sedimentary  
222 successions (i.e., WMAR/SWAL seismic sources in Figure 3). The position of the boundary  
223 between these sources was primarily defined from interpretations of regional gravity,  
224 magnetic anomalies, geological mapping, and to a lesser extent the distribution of seismicity.  
225 The best estimate position, based on the weight of evidence from all of the above, was  
226 represented by the SSMs with a northern boundary position (SSM-A, SSM-B, SSM-C and  
227 SSM-D). Epistemic uncertainty was captured by the inclusion of alternative SSMs with a  
228 southern boundary position located 10 km to the south (SSM-E and SSM-F). At its closest,  
229 this boundary is located either 12 km from the site (southern position) or 22 km from the site  
230 (northern position).

231 The second most important source of uncertainty was the definition of the seismic source  
232 enclosing the higher level of seismicity observed in South Wales. Four different theories were  
233 postulated which could explain this higher level of seismicity:

- 234 • Seismicity is associated with the Wrekin Terrane (WMAR-A, WMAR-E) and the  
235 increased seismicity in South Wales is due to chance.
- 236 • The increased seismicity in South Wales is associated with a stronger tectonic fabric  
237 imparted by the Variscan Orogeny on the southern part of the Wrekin Terrane (SWAL-B,  
238 SWAL-E), and this fabric is not present across the remainder of the terrane (WMAR-B,  
239 WMAR-F).
- 240 • The increased seismicity is associated with the Welsh Coalfield (SWAL-C), leaving a  
241 residual zone encompassing the remainder of the terrane (WMAR-C).
- 242 • The increased seismicity is associated with clustering in the Swansea area due to the  
243 intersection of major faults (SWAL-D), leaving a residual zone encompassing the  
244 remainder of the terrane (WMAR-D).

245



246

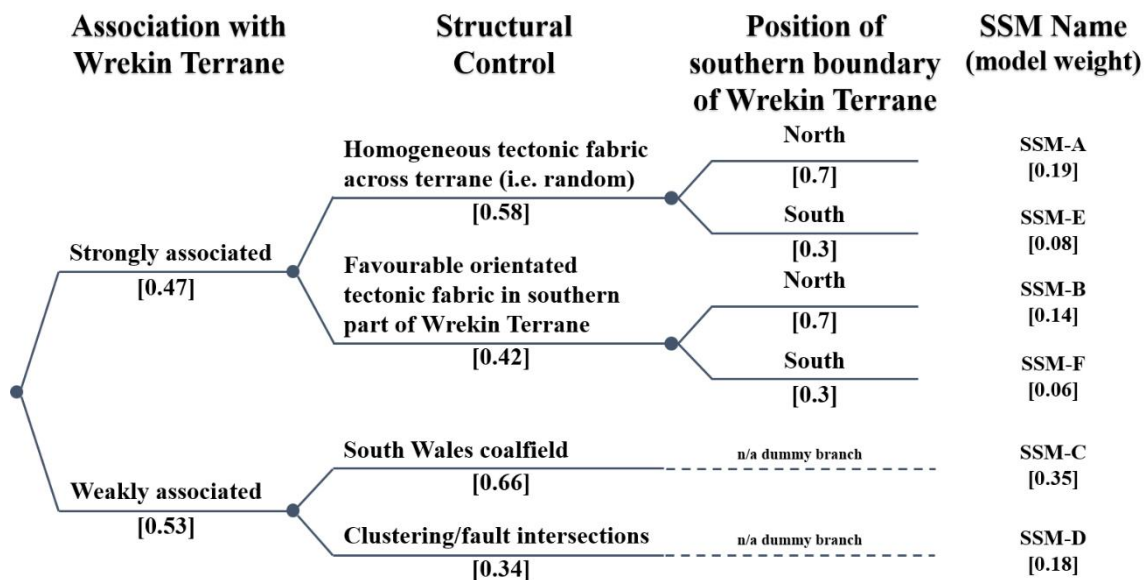
247

248

249

**Fig. 3** Seismic source models (SSM) A to F coloured areas indicate those seismic sources with geometries which vary across the various SSMs, greyed sources have constant geometries for all models

250 The consideration of these uncertainties through a logic tree framework resulted in the six  
 251 SSMs shown in Figure 3. Only area sources were included in the SSMs, as there was  
 252 insufficient evidence to support the inclusion of any seismogenic faults (i.e. distinct  
 253 seismogenic features that would be the focus of future seismic activity) in the source models.  
 254 This conclusion is consistent for a site that occurs in a low, relatively homogenous, tectonic  
 255 stress regime, which has only experienced low to moderate levels of seismicity. The resulting  
 256 logic tree and weights assigned to each alternative branch are shown in Figure 4. The process  
 257 for the weighting of the logic tree resulted in assigning almost equal weights to the two  
 258 hypotheses of the strength of the association with the Wrekin Terrane. However, it is likely  
 259 that the effect on the hazard of weighting them equally (both at 0.5) as opposed to 0.53 and  
 260 0.47 would be small.



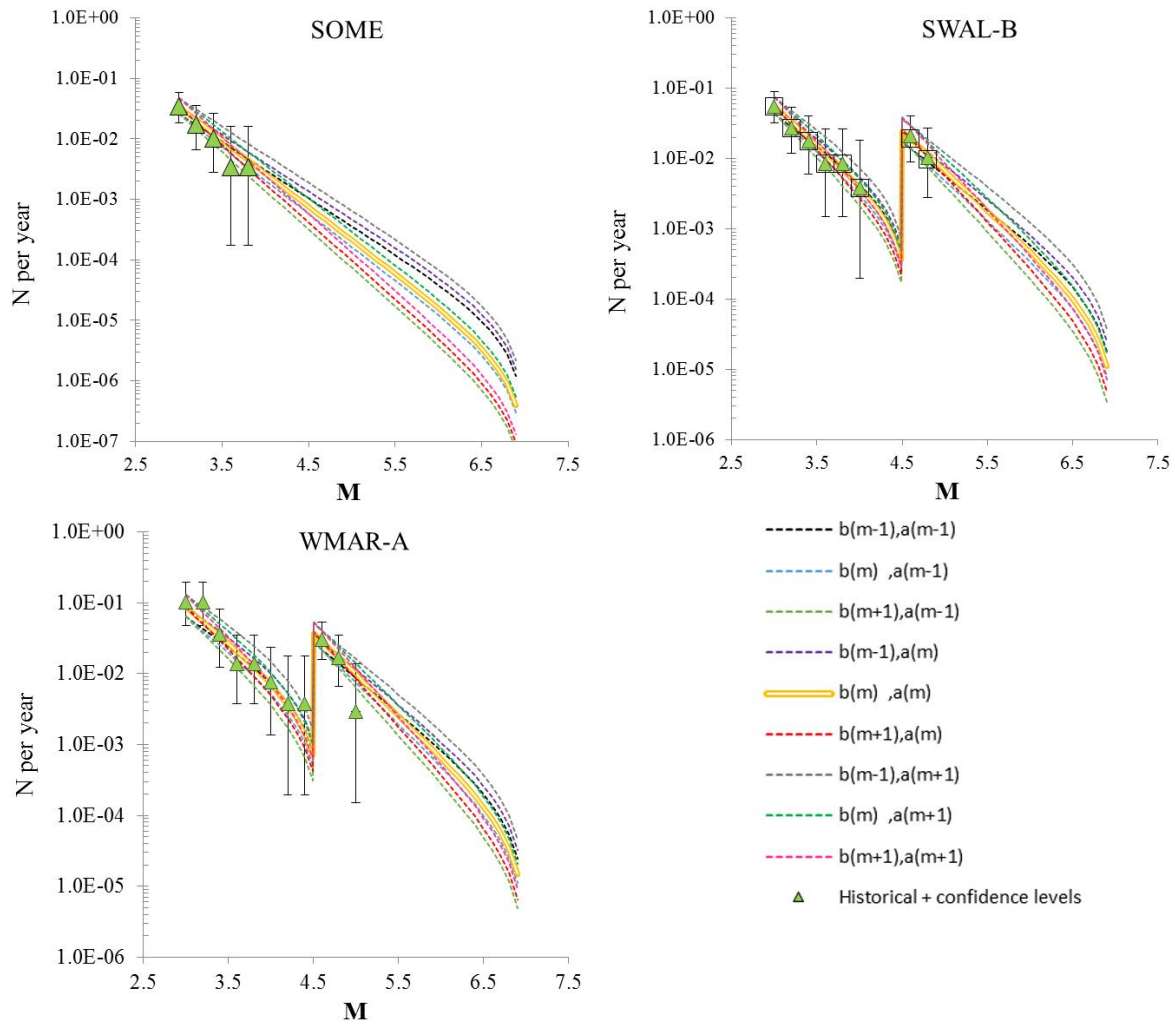
261  
 262 **Fig. 4** Seismic source model logic tree for source zonation. Numbers in square brackets are weights  
 263 assigned to each alternative branch

### 264 3.2. Seismic Source Zones Parameterization

265 Recurrence rates were determined for all the seismic source zones considering the  
 266 doubly-truncated exponential Gutenberg-Richter model. To capture epistemic uncertainties  
 267 associated with the activity rate (a) and b-value parameters characterizing the Gutenberg-  
 268 Richter relation, the logic-tree considered nine combinations of a and b values (three values  
 269 for a, three values for b, with the three values comprising the central estimate, and the central  
 270 estimate plus and minus one standard deviation) for the host seismic source (SOME) and the  
 271 two seismic sources in southern Wales (SWAL and WMAR), which were identified as the  
 272 most hazard-significant seismic sources in the model. The weights for these alternative (a, b)

273 combinations were source-specific as they were based on a maximum-likelihood fit to the  
 274 data in each source. Calculations were performed using the penalized maximum likelihood  
 275 method (EPRI 1994), which ensures that the complete space of possible (a,b) combinations is  
 276 captured and weighted appropriately (i.e., considering that the uncertainty in a and b are  
 277 correlated). For all other seismic sources, a single best estimate (a, b) combination was  
 278 adopted with a weight of 1.0.

279 Three values of  $M_{\max}$  were assigned:  $M$  6.5, 6.8 and 7.1, with respective weights of 0.5,  
 280 0.4 and 0.1. These  $M_{\max}$  values and corresponding weights represent a simplified version of  
 281 those proposed for the British Isles by Meletti et al. (2010) as part of the SHARE project  
 282 (Woessner et al. 2015). Cumulative earthquake magnitude rates for the most hazard-  
 283 significant sources (only one variant of the SWAL and WMAR sources are presented due to  
 284 space limitations), considering all (a,b) combinations and  $M_{\max} = 7.1$  are shown in Figure 5.



285

286 **Fig. 5** Cumulative earthquake rates for the three most hazard-significant sources, and for  $M_{\max} =$   
287 6.8.  $a(m)$  and  $b(m)$  correspond to the central  $a$  and  $b$  values,  $a(m+1)$  and  $a(m-1)$ , and  $b(m+1)$  and  $b(m-$   
288 1), correspond to the central  $a$  and  $b$  values plus and minus one standard deviation, respectively

289 For the seismic sources covering the South Wales region, a departure from the  
290 exponential distribution assumed by the Gutenberg-Richer model was observed for  
291 magnitudes below  $M$  4.5 (see Figure 5). This type of seismicity has been referred to as “semi-  
292 characteristic” seismicity by Musson and Sargeant (2007), who confronted a similar feature  
293 during the preparation of the UK national seismic hazard maps. This is explained as the  
294 presence of a bipartite magnitude-frequency distribution (Musson 2015).

295 The minimum magnitude ( $M_{\min}$ ) to be used in the hazard calculations is not specified by  
296 the UK regulator. This parameter defines the lower limit of integration over earthquake  
297 magnitudes such that using a smaller value would not alter the estimated risk to the structure  
298 under consideration (Bommer and Crowley 2017) and has traditionally been set to  $M$  4.0 in  
299 UK nuclear-safety-related seismic hazard studies. For the host source (SOME)  $M_{\min}$  was  
300 taken as  $M$  4.0, consistent with this precedent. For all other sources, a pragmatic decision was  
301 taken to increase  $M_{\min}$  from  $M$  4.0 to  $M$  4.5. This simplifies the modelling of the earthquake  
302 recurrence model in view of the bipartite magnitude-frequency distribution discussed above,  
303 which otherwise would result in unnecessarily increased complexity of the hazard  
304 calculations, since the difference in  $M_{\min}$  has a negligible impact on the hazard. Indeed,  
305 sensitivity calculations showed that the contribution to the total hazard from earthquakes  $< M$   
306 4.5 outside the host zone was about 0.2%.

307 A common hypocentral depth ( $h$ ) distribution was assumed for all seismic sources. This  
308 took the form of a discrete aleatory distribution, for depths between 5 and 25 km, reflecting  
309 the relative frequencies of occurrence estimated from the hypocentral distribution of the  
310 seismicity larger than  $M$  4.

311 All seismic sources were modelled as area sources at specific depths; no linear fault  
312 sources were considered. Earthquake occurrences within the seismic sources were modelled  
313 using the “floating earthquake” concept, where a spatially uniform distribution of the  
314 earthquake epicenters is assumed, in combination with virtual fault ruptures. The simulated  
315 fault rupture characteristics were based on knowledge of the existing geological structure,  
316 earthquake focal mechanisms and the current stress regime. All virtual fault ruptures were  
317 assumed to occur on vertical fault planes, hypocenters were assumed to be located centrally  
318 (both along-strike and along-dip) of the virtual rupture plane, and the concept of leaky

319 boundaries was assumed for all sources. The fault rupture plane in CRISIS2015 is fixed to a  
320 circular shape, which gives a 1:1 aspect ratio. The extent of the virtual fault ruptures was  
321 magnitude dependent, calculated using the area scaling relationship for stable continental  
322 regions of Leonard (2010). Randomization of the rupture area was not considered. The  
323 orientation of the virtual fault ruptures was common to all sources, but specific to the style-  
324 of-faulting assumed; when multiple rupture orientations were possible, these were modelled  
325 as a discrete aleatory distribution of strike angles with associated relative frequencies.  
326 Earthquake occurrence for all seismic sources was modelled using the double-truncated  
327 exponential Gutenberg-Richter model.

#### 328 **4. Ground-motion Model (GMM)**

329 A rigorous and systematic approach was followed to develop a site-specific GMM for the  
330 HPC site. In line with state-of-the-practice PSHAs for high-value infrastructure, the site-  
331 specific GMM for the Hinkley PSHA comprised two separate models, the median ground-  
332 motion model and the aleatory variability (sigma) model. The GMM was developed to  
333 predict ground motions for the  $V_{S30}$  at the reference velocity horizon and then near-surface  
334 effects due to the shallow deposits were accounted for through a hazard-compatible site  
335 response analysis (see Site Response Analysis section below). In agreement with the  
336 principle of a site-specific PSHA, a partially non-ergodic sigma model was adopted (i.e., a  
337 sigma model where the site-to-site variability, normally included in the intrinsic sigma  
338 models of the GMPEs, is removed; Rodriguez-Marek et al. 2013).

##### 339 **4.1. Median Ground-motion Model**

340 Traditionally in PSHA, epistemic uncertainty within ground-motion prediction is captured  
341 by selecting a suite of candidate GMPEs, which are considered to provide an adequate  
342 prediction of the ground-motion scaling in the region of interest. This approach can be  
343 referred to as the “traditional” or “multi-GMPE” approach. However, some recent studies  
344 have championed an alternative approach, normally referred to as “backbone” approach,  
345 where fewer GMPEs than in the traditional approach are selected (normally one or two) and  
346 epistemic uncertainty is captured by scaling up or down the median predictions of the  
347 selected GMPEs (e.g. Bommer 2012; Atkinson et al. 2014; Douglas 2018).

348 After careful consideration of the advantages and disadvantages of both approaches, the  
349 GMM team opted for the multi-GMPE approach for the Hinkley PSHA. It was thought that  
350 the backbone approach would require significant additional work, mainly associated with the

351 higher level of detail needed for the selection of the most appropriate GMPE for the region  
352 and for the calibration of the scaling of the selected GMPE required to account for the  
353 uncertainty on, for example, the median stress drop of UK earthquakes. It was also thought  
354 that the number of selected GMPEs for the project (five) from different geographical regions  
355 (including a GMPE from the UK itself), combined with the alternative  $V_S$ -kappa adjustments  
356 to their median predictions (upper, middle and lower adjustment factors), accounted for the  
357 epistemic uncertainty (also see Median Ground Motion Logic Tree sub-section below).

#### 358 **4.1.1. Approach to Selection of GMPEs**

359 A critical review and comparison of an initial list of GMPEs was carried out to identify a  
360 final set of suitable candidate GMPEs for the Hinkley PSHA. At the first stage of the  
361 selection process over 400 potential candidate GMPEs were identified from the online  
362 compendium of Douglas (2014). This was reduced to a shortlist of 12 GMPEs by applying  
363 selection criteria based on recommendations by Cotton et al. (2006) and Bommer et al.  
364 (2010). Consideration was also given to selection criteria used in previous high-level seismic  
365 hazard studies [e.g., PEGASOS Refinement Project (Renault 2014); GEM Global GMPEs  
366 project (Douglas et al. 2012; Stewart et al. 2015)]. An assessment of the 12 preliminary-  
367 selected GMPEs was carried out by comparing the ground-motion predictions from the  
368 various models, as well as comparisons against ground-motion instrumental and intensity  
369 data retrieved as part of this project. Due to limitations of the instrumental and intensity data,  
370 comparisons against observations provided only limited, qualitative, guidance for the  
371 selection of the final suite of candidate GMPEs. For this reason, quantitative methods for the  
372 assessment of the match between ground-motion predictions from the GMPEs and  
373 instrumental data (e.g., Scherbaum et al. 2004, 2009) were not applied.

374 The selection of the final suite of candidate GMPEs was done through an expert  
375 judgement assessment by the GMM team based on a set of criteria that considered a range of  
376 pertinent technical issues, including the comparisons of the ground-motion predictions from  
377 the various models amongst themselves and against the ground-motion data, and project-  
378 specific factors. Based on this process, five GMPEs were selected for the prediction of the  
379 median ground-motion:

- 380 • Atkinson and Boore (2006, 2011) [AB0611] – model for ‘hard rock’ ( $V_{S30} > 2,000$  m/s);
- 381 • Bindi et al. (2014a, b) [BETAL14] – model using  $R_{JB}$  and  $V_{S30}$ ;
- 382 • Boore et al. (2014) [BOOREETAL14] – base model (i.e., without regional factors);

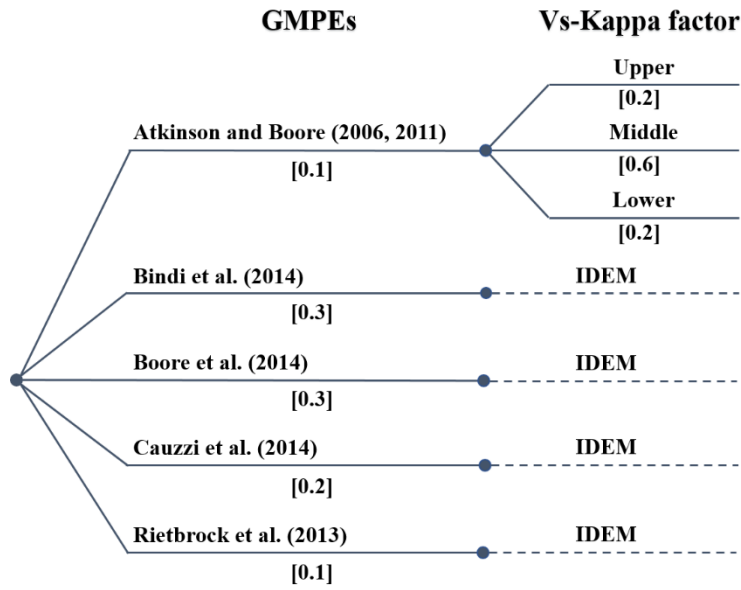
- 383 • Cauzzi et al. (2015) [CETAL15] – considering the period-dependent reference  $V_{S30}$ ;  
384 • Rietbrock et al. (2013) [RETAL13d] – magnitude-dependent stress drop model.

385 These models were subsequently adjusted to predict median ground-motions compatible  
386 with the ground conditions at the reference velocity horizon level defined for the HPC site  
387 (i.e.,  $V_S$ -kappa adjustments) and to address incompatibility issues between dependent  
388 parameters of the various GMPEs, specifically style-of-faulting.

389 For the exploration of the space occupied by the suite of GMPEs methods such as the  
390 Sammon’s map approach (Scherbaum et al. 2010; Scherbaum and Kuehn 2011) were  
391 considered. However, in view of project constraints, a full application of the Sammon’s map  
392 technique and related visualization methods were considered beyond the scope of the study.  
393 Instead, a model-based approach was implemented for the weighting of the alternative  
394 GMPEs using the arguments for and against the various selected GMPEs considered during  
395 the GMPEs selection process.

396 The GMM team’s degree-of-confidence in the various selected GMPEs resulting from  
397 this process was relatively uniform, which resulted on an a priori assessment of equal  
398 weights. However, it was decided to assign lower weights to the stochastic models in view of  
399 the important contributions to the hazard expected from the close-in sources, as they are  
400 known to be poorly constrained at short distances. The weight subtracted from the stochastic  
401 models was redistributed equally between the BETAL14 and BOOREETAL14 models,  
402 which were considered the overall best-behaved GMPEs in the selection. The CETAL15  
403 equation thus is assigned a lower weight than the other two empirical GMPEs. This reflects  
404 the fact that CETAL15 is considered less well constrained than the BETAL14 and  
405 BOOREETAL14 models. Additionally, the underlying database of CETAL15 has not been  
406 subjected to the same level of scrutiny as the NGA-West 2 and RESORCE databases used by  
407 Boore et al. (2014) and Bindi et al. (2014a,b).

408 The final weighting scheme for the GMPE is shown in the Median Ground Motion logic  
409 tree in Figure 6.



410

411 **Fig. 6** Median ground-motion logic tree for the Hinkley PSHA. Numbers in square brackets are the  
 412 weights assigned to each alternative branch

413 **4.1.2.  $V_S$ -kappa Adjustment Factors**

414 Following the selection of the final suite of GMPEs, the median predictions of each  
 415 GMPE had to be adjusted to account for differences between the host region for which the  
 416 GMPE was derived and the target location corresponding to the study site. This host-to-target  
 417 adjustment involved quantifying, for the host and target regions, the effects of the shallow  
 418 crustal shear-wave velocity ( $V_S$ ) and the high-frequency crustal attenuation, termed “kappa”.

419 The calculation of the  $V_S$ -kappa adjustment required four inputs to be defined:

- 420 • Average  $V_S$  profiles of the host ( $V_{S\text{-host}}$ ) and target ( $V_{S\text{-target}}$ ) locations; and  
 421 • Average kappa in the host ( $\text{kappa}_{\text{host}}$ ) and target ( $\text{kappa}_{\text{target}}$ ) locations.

422 For the two stochastic models (i.e. AB0611 and RETAL13d)  $V_{S\text{-host}}$  profiles were  
 423 evaluated using information provided by the developers of these models. For the three  
 424 empirical models (BETAL14, BOOREETAL14 and CETAL15),  $V_{S\text{-host}}$  profiles were derived  
 425 using the generic  $V_S$  profiles of Cotton et al. (2006) for a  $V_{S30}$  value of 1,000 m/s.

426 For each GMPE,  $\text{kappa}_{\text{host}}$  values were estimated using an approach involving generation  
 427 of Fourier amplitude spectra for a scenario earthquake obtained from disaggregation using  
 428 inverse random vibration theory (IRVT, Al Atik et al. 2014). The sensitivity of the kappa  
 429 value to the earthquake magnitude and distance and to the fitted frequency range was  
 430 investigated in some detail. It was found that for some GMPEs the kappa values depended  
 431 quite significantly on magnitude and distance. Rather than propagate this additional

432 computational load through the hazard calculation (which would also make checking of the  
433 calculations more difficult) and because some of the kappa values obtained from the  
434 inversion for some scenarios were unphysical, a single scenario was chosen based on  
435 controlling earthquake scenarios obtained from preliminary seismic hazard calculations for  
436 the HPC site for the high-frequency range, where the  $V_S$ -kappa adjustment factors are more  
437 important.

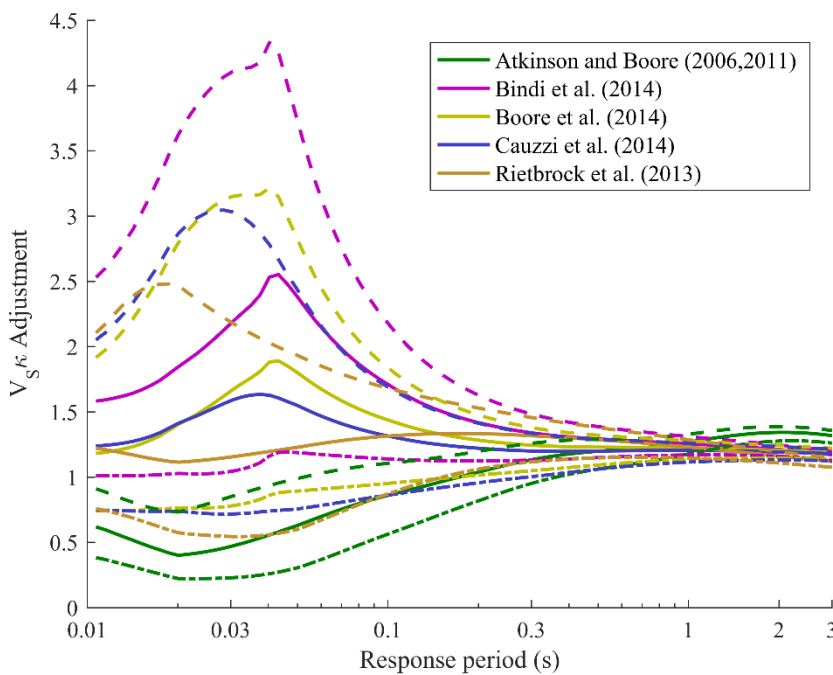
438 The  $V_{S\text{-target}}$  profile was developed based on information obtained from a variety of  
439 sources, including: shallow borehole seismic data (down to approximately 120 m) available  
440 from the various historical ground investigation campaigns at the site, published velocity data  
441 from the 1 km deep Burton Row borehole (located 13 km ENE of the Hinkley Point site and  
442 which penetrates the same geological sequence), two crustal velocity models derived for the  
443 HPC site by SHWP (1987) using recordings from the Hinkley Point microseismic network,  
444 and the published deep crustal velocity model of Hardwick (2008) from local earthquake  
445 tomography.

446 A single  $V_{S\text{-target}}$  profile was ultimately defined using a curve-fitting approach based on  
447 the method of Cotton et al. (2006). Whilst the shear-wave velocity at the Hinkley Point  
448 reference velocity horizon has a value of 1,000 m/s, the  $V_{S30}$  of the target  $V_S$  profile was  
449 1,077 m/s.

450 Considerable efforts were expended trying to define a  $\kappa_{\text{target}}$  based on data available  
451 from the Hinkley Point microseismic network installed and operated by the SHWP from 1985  
452 to 1994. However, the kappa values obtained for most stations examined were found to be  
453 compromised by potential site effects. The few ‘unaffected’ kappa values from the remaining  
454 stations were subsequently considered to be less relevant, due to the proposed definition of  
455 the reference velocity horizon at some depth beneath the site. Estimating  $\kappa_{\text{target}}$  from the  
456 microseismic data was, therefore, not considered possible for the study. These few surface  
457 kappa estimates could have been combined with the low-strain damping used in the site  
458 response analyses to derive estimates of kappa at the reference velocity horizon but this was  
459 not attempted in view of the large dispersion in the estimates.

460 Following a literature review of kappa estimates from UK earthquake data, it was decided  
461 to use the empirical relationship of Van Houtte et al. (2011) to provide a best-estimate  
462  $\kappa_{\text{target}}$  derived from the target  $V_{S30}$  value of 1,077 m/s. To account for the epistemic  
463 uncertainty on the estimation of  $\kappa_{\text{target}}$ , three logic tree branches were set up to cover

464 upper bound, best-estimate and lower bound values (0.0342 s, 0.0197 s and 0.0114 s,  
 465 respectively), where the upper and lower bounds were set equal to the best-estimate value  $\pm 1$   
 466 standard deviation defined by Van Houtte et al. (2011). Weights to each alternative  $\kappa_{\text{target}}$   
 467 branch were assigned following a three-point approximation to the normal distribution as  
 468 shown in Figure 6. The best-estimate  $\kappa_{\text{target}}$  value (middle branch) estimated for HPC  
 469 compared well with  $\kappa$  estimates for rock sites in the UK provided by Rietbrock et al.  
 470 (2013), Ottemöller et al. (2009) and Ottemöller and Sargeant (2010). The variation of the  
 471 final adjustment factors with period for all five GMPEs and the three alternative  $\kappa_{\text{target}}$   
 472 values are shown in Figure 7.



473  
 474 **Fig. 7**  $V_S$ - $\kappa$  adjustment factors for application to response spectral acceleration from the host  
 475 GMPEs for the target  $V_S$  profile and  $\kappa$  values. Solid lines are for the middle target  $\kappa$ , dashed  
 476 lines correspond to the lower target  $\kappa$  and the dash-dotted lines correspond to the upper target  
 477  $\kappa$

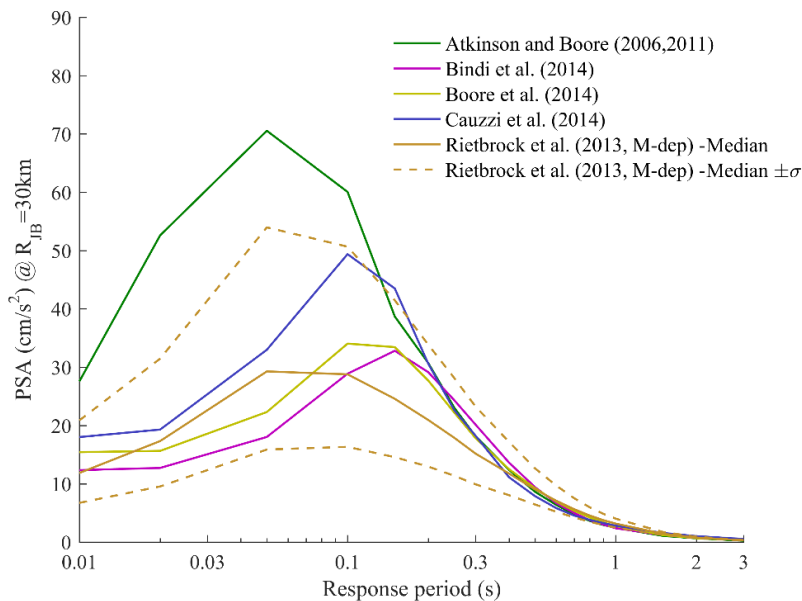
### 478 4.1.3. Median Ground Motion Logic Tree

479 The median ground-motion model for the Hinkley PSHA is then the result of combining  
 480 the selected GMPEs and their corresponding  $V_S$ - $\kappa$  adjustment factors through the logic  
 481 tree framework as represented in Figure 6. This median ground-motion model represents, in  
 482 the view of the GMM team, the best ground-motion model for the specific region of interest  
 483 (i.e., within 300 km of the HPC site).

484 Epistemic uncertainty in the median ground-motion model is captured by the two levels  
 485 of logic-tree branches (i.e., GMPEs and  $V_S$ - $\kappa$  factors). The rigorous selection of the

486 candidate GMPEs, along with the range of site-specific  $V_S$ -kappa adjustment factors, and  
 487 corresponding weights, provides confidence that the median ground-motion model captures  
 488 the range of likely ground-motion intensities (i.e., epistemic uncertainty) at the HPC site.

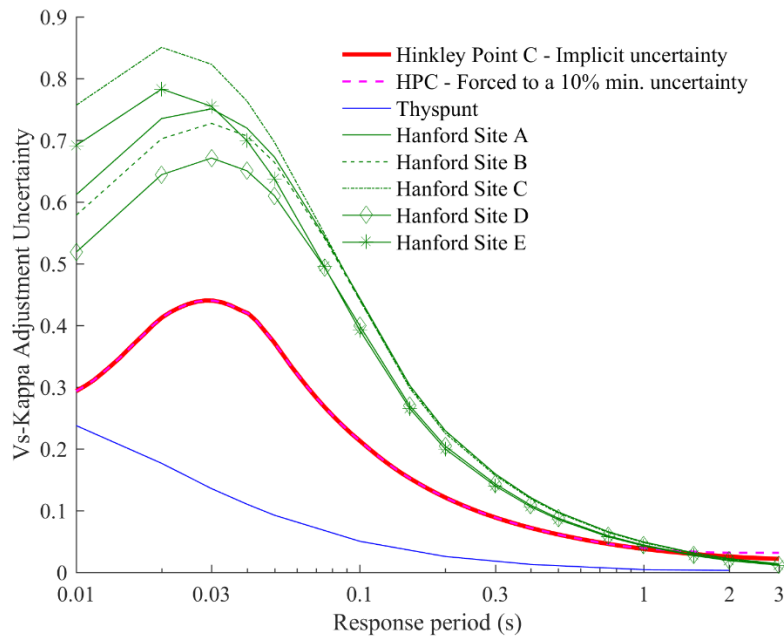
489 A comparison of the ground motions predicted by the five selected GMPEs against the  
 490 magnitude-dependent model of Rietbrock et al. (2013), modified to account for a variation in  
 491 the median stress parameter of  $\pm 1\sigma(\log_{10}[\Delta\sigma])$  (i.e., 4 to 25.1 MPa, with a median of 10  
 492 MPa), shows that the suite of selected GMPEs adequately captures the epistemic uncertainty  
 493 regarding the appropriate value of the stress parameter for the UK (see Figure 8). Previous  
 494 studies present evidence that stress parameter increases with magnitude hence it could be  
 495 argued that the upper bound of potential stress parameters for large UK earthquakes could be  
 496 higher than the 25.1 MPa assumed in Figure 8. This figure shows, however, that the GMPE  
 497 of Atkinson and Boore (2006, 2011) would still envelope the adjusted Rietbrock et al. (2013)  
 498 GMPE at short structural periods even for higher median stress parameters.



499  
 500 **Fig. 8** Comparison of the response spectra for  $R_{JB} = 30$  km and  $M = 5.0$  from the finally selected  
 501 GMPEs, the Rietbrock et al. (2013) magnitude-dependent model for median stress parameter (10  
 502 MPa) and the median  $\pm 1$  logarithmic standard deviation of the stress parameter (i.e., 4 and 25.1 MPa)

503 The level of uncertainty implicit in the adjustment factors developed for the Hinkley  
 504 PSHA was estimated and compared against uncertainty values reported for similar studies  
 505 [i.e., Thyspunt project (Rodriguez-Marek et al. 2014); and Hanford project (Coppersmith et  
 506 al. 2014)]. Uncertainty levels implicit in the Hinkley PSHA  $V_S$ -kappa adjustment factors for  
 507 periods below 0.1 sec were found to be midway between the Thyspunt and Hanford

508 uncertainty levels, for periods above 0.1 s Hinkley PSHA and Hanford uncertainty levels  
 509 were found to be similar (see Figure 9). The intrinsic uncertainty captured in the  $V_S$ -kappa  
 510 adjustment factors presented in Figure 9 was computed similarly to Rodriguez-Marek et al.  
 511 (2014) as the weighted sample standard deviation of the logarithmic  $V_S$ -kappa adjustment  
 512 factors shown in Figure 7.



513  
 514 **Fig. 9** Uncertainty implicit in the  $V_S$ -kappa adjustment factors for the HPC project compared to the  
 515 equivalent values from the Thyspunt project (Rodriguez-Marek et al. 2014) and the Hanford project  
 516 (Coppersmith et al. 2014). The dashed line for HPC corresponds to the case where the adjustment  
 517 factors are forced to have a minimum spread of 10% around the best estimate value to account for  
 518 unaccounted epistemic uncertainty on the target  $V_S$  profile. All values are given in terms of the natural  
 519 logarithm

## 520 4.2. Sigma Model

521 The sigma model for the Hinkley PSHA was based on the single-station sigma ( $\sigma_{SS}$ )  
 522 concept. The application of this concept within a PSHA for a nuclear power plant is presented  
 523 by Rodriguez-Marek et al. (2014). The  $\sigma_{SS}$  model developed for the Hinkley PSHA considers  
 524 separate models for the inter-event variability ( $\tau$ ) and the single-station intra-event variability  
 525 ( $\phi_{SS}$ ), adjusted by a partially ergodic site-to-site variability term ( $\delta\phi_{S2S}$ ) which accounts for  
 526 epistemic uncertainty unaccounted for in the  $V_S$ -kappa adjustment factors, as well as the  
 527 amplification factors considered in the site response. Both the  $\phi_{SS}$  and  $\tau$  models for the  
 528 Hinkley PSHA were taken from models available in literature.  $\delta\phi_{S2S}$  was calculated by  
 529 forcing the uncertainty implicit in the  $V_S$ -kappa adjustment factors to remain above 10%  
 530 across all response periods.

531 **4.2.1. Tau Model**

532 Following a comparison and assessment of eight tau ( $\tau$ ) models, the  $\tau$  model of  
533 Abrahamson et al. (2014) was selected. To account for the epistemic uncertainty on whether  
534 the observed inter-event variability of the ground motion is magnitude-dependent or not,  
535 which is still an unresolved issue within the technical community, two alternative branches  
536 for the  $\tau$  logic tree were considered. The first of the branches considered the magnitude-  
537 dependent (heteroscedastic)  $\tau$  model of Abrahamson et al. (2014), while the second branch  
538 considered a magnitude-independent (homoscedastic)  $\tau$  model, which was taken as the  
539 Abrahamson et al. (2014)  $\tau$  model evaluated for  $M \leq 6.0$ . The weights assigned to these  
540 alternative branches are discussed in the Sigma Logic Tree sub-section below.

541 A second level of branches in the  $\tau$  model logic tree was considered to account for the  
542 epistemic uncertainty on the median  $\tau$  predictions of each of the two alternative models (i.e.,  
543 heteroscedastic and homoscedastic models). The second level of branches in the  $\tau$  model  
544 logic tree considered upper and lower branches, in addition to the median branch, which were  
545 defined so as to envelope roughly the other examined  $\tau$  models for magnitudes of less than  
546  $M \leq 6.0$ . For this second level of branches, weights were selected in accordance with the  
547 three-point representation of the normal distribution.

548 **4.2.2.  $\phi_{SS}$  Model**

549 In a similar manner as for the  $\tau$  model, various  $\phi_{SS}$  models available in literature were  
550 assessed. Based on this assessment a  $\phi_{SS}$  model logic tree for the Hinkley PSHA was  
551 developed considering the constant and magnitude-dependent models of Rodriguez-Marek et  
552 al. (2013). The first level of branches on the  $\phi_{SS}$  logic tree considered the epistemic  
553 uncertainty on the magnitude-dependency of the intra-event variability of the ground motion  
554 (i.e., heteroscedastic and homoscedastic models). The heteroscedastic  $\phi_{SS}$  model for the  
555 Hinkley PSHA was defined as a hybrid model consisting of taking the larger  $\phi_{SS}$  estimate of  
556 the constant and magnitude-dependent models of Rodriguez-Marek et al. (2013). The  
557 homoscedastic  $\phi_{SS}$  model was taken as the constant model of Rodriguez-Marek et al. (2013).

558 The second level of branches in the  $\phi_{SS}$  logic tree addressed the epistemic uncertainty  
559 associated with the median estimates of the  $\phi_{SS}$  models (i.e., heteroscedastic and  
560 homoscedastic) by including upper and lower branches. The upper and lower branches were  
561 constructed using the same dispersion in the median  $\phi_{SS}$  prediction ( $\phi_{SS,S}$ ) as estimated by

562 Rodriguez-Marek et al. (2014), which led to branches at  $1.16 \phi_{SS}$ ,  $\phi_{SS}$  and  $0.84 \phi_{SS}$ . Weights  
563 were assigned to each branch in accordance with the three-point representation of the normal  
564 distribution. It should be noted that the theoretically-more-appropriate chi-square distribution  
565 was used in some recent studies (e.g. Coppersmith et al., 2014).

#### 566 **4.2.3. Partially Ergodic Correction Term at Reference Horizon, $\delta\phi_{S2S}$**

567 One of the requirements for the application of the single-station sigma concept is that  
568 epistemic uncertainty in the site term should be duly considered (Rodriguez-Marek et al.  
569 2014; Coppersmith et al. 2014). This section deals more specifically with the site term at the  
570 reference velocity horizon, which in the Hinkley PSHA median GMM is represented by the  
571 suite of  $V_s$ -kappa adjustment factors presented earlier. The implicit uncertainty associated  
572 with this suite, shown in Figure 9, represents the total epistemic uncertainty captured in the  
573  $V_s$ -kappa adjustment model, combining the epistemic uncertainty in the target kappa values,  
574 with the epistemic uncertainty captured by starting from a range of GMPEs, since all host-  
575 target combinations were considered. For HPC, the range of host kappas is very broad,  
576 ranging from very low values representative of CEUS to high values typical of active regions.  
577 It was therefore assessed that epistemic uncertainties were adequately captured in terms of  
578 the kappa contribution.

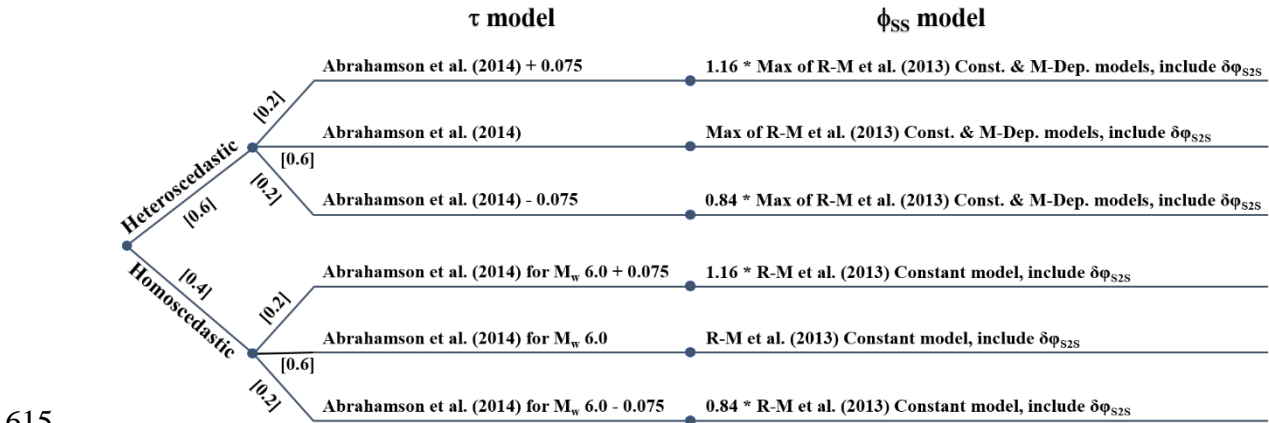
579 However, since the  $V_s$ -kappa adjustment considered a single target  $V_s$  profile, it was felt  
580 following discussions with Subject Experts that a correction factor to account for the  
581 epistemic uncertainty in this profile ought to be included in the site term at the reference  
582 horizon. Previous studies have found that the uncertainty relating to the selection of the target  
583  $V_s$  profile accounts for up to 10% of the epistemic variability intrinsic to a suite of  $V_s$ -kappa  
584 adjustment factors (Biro and Renault 2012). Therefore, the adjustment factors at longer  
585 periods were modified such that the lower and upper adjustment factors for each GMPE  
586 deviated by at least 5% from the median adjustment factor, resulting in an overall minimum  
587 spread of 10%. The  $\delta\Phi_{S2S}$  factor was then calculated based on the absolute difference  
588 between modified and original  $V_s$ -kappa adjustment factor uncertainty, and applied as a  
589 partially ergodic correction factor to the  $\phi_{SS}$  term of the total ground-motion variability at the  
590 reference horizon as in Rodriguez-Marek et al. (2014).

591 **4.2.4. Sigma Logic Tree**

592 The total sigma logic tree considered alternative branches for heteroscedastic and  
 593 homoscedastic variability in the first level of the logic tree. In the second level of the logic  
 594 tree, upper and lower branches were considered in addition to the mean branch to account for  
 595 epistemic uncertainty associated with the median predictions. The total-sigma upper, median  
 596 and lower branches were constructed by combining upper-upper, median-median and lower-  
 597 lower branches of the proposed  $\phi_{SS}$  and the  $\tau$  models, for the heteroscedastic and  
 598 homoscedastic parts of the logic tree, independently. We chose this approach, the same as  
 599 followed by Bommer et al. (2015), although different to that of Coppersmith et al. (2014)  
 600 who combine the variances, to simplify the model. Combining upper-upper, median-median  
 601 and lower-lower branches of the  $\tau$  and  $\phi_{SS}$  is deemed sufficiently equivalent to considering all  
 602 combinations, and resampling the logic-tree accordingly, as both the center and the range of  
 603 sigma values remain the same although a slightly wider range of epistemic uncertainty is  
 604 modelled. The total single-station sigma ( $\sigma_{SS}$ ) logic tree for the Hinkley PSHA is presented in  
 605 Figure 10. The single-station sigma,  $\sigma_{SS}$ , for each branch of the logic tree in then calculated  
 606 using the following equation:

607 
$$\sigma_{SS} = \sqrt{\tau^2 + \phi_{SS}^2 + \delta\phi_{SS}^2} \quad (1)$$

608 Weights of 0.4 and 0.6 were assigned to the homoscedastic and heteroscedastic branches,  
 609 respectively. This reflects the state-of-knowledge, with heteroscedastic between-event  
 610 variability being often observed empirically and generally considered to be physically  
 611 justifiable; however, doubt remains on whether this is a sampling issue or due to poorer-  
 612 constrained parameters for smaller events (Al Atik 2014). For the second level of branches,  
 613 weights of 0.2, 0.6 and 0.2 were adopted for the upper, median and lower branches,  
 614 respectively, in line with the weights assigned to the branches of both the  $\tau$  and  $\phi_{SS}$  models.



615

616 **Fig. 10** Total sigma logic tree for the Hinkley PSHA. Numbers in square brackets are weights  
617 assigned to each alternative branch

## 618 **5. Seismic Hazard at Reference Velocity Horizon**

619 This section presents a summary of the methodology implemented to perform the hazard  
620 calculations for the Hinkley PSHA and the resulting hazard estimates at the reference  
621 velocity horizon. The latter formed part of the input data required for the site-response  
622 analysis, and were considered representative of both the onshore and offshore domains.

### 623 **5.1. Seismic Hazard Methodology**

624 Seismic hazard calculations were undertaken using the standard Cornell-McGuire  
625 approach (Cornell 1968; McGuire 1976), including explicit treatment of the epistemic  
626 uncertainty, using the logic-tree framework (Kulkarni et al. 1984), and aleatory variability of  
627 the ground motion.

628 The main seismic hazard calculations were performed using the software CRISIS2015  
629 v1.0 (Ordaz et al. 2015). In addition to CRISIS2015 v1.0, the OpenQuake engine (OQ-  
630 engine, Pagani et al. 2013) was used as an alternative software to perform cross-checking  
631 calculations on a selected sub-set of the final hazard calculations as part of the QA process,  
632 following the approach of Bommer et al. (2013). Both programs include most of the modern  
633 features expected in seismic hazard software packages such as disaggregation analysis, leaky  
634 source boundaries and virtual fault ruptures.

635 Epistemic uncertainty was incorporated in the hazard calculations through the  
636 implementation of the logic tree framework. CRISIS2015 allows for the use of logic trees;  
637 however, for the Hinkley PSHA it was not possible to evaluate the logic tree using  
638 CRISIS2015 due to the very large number of branches. Output files of the hazard calculations  
639 at the end tip of each branch of the logic tree were compiled separately for each source zone,  
640 with logic tree calculations carried out at the post-processing stage using Matlab codes  
641 developed specifically for this project.

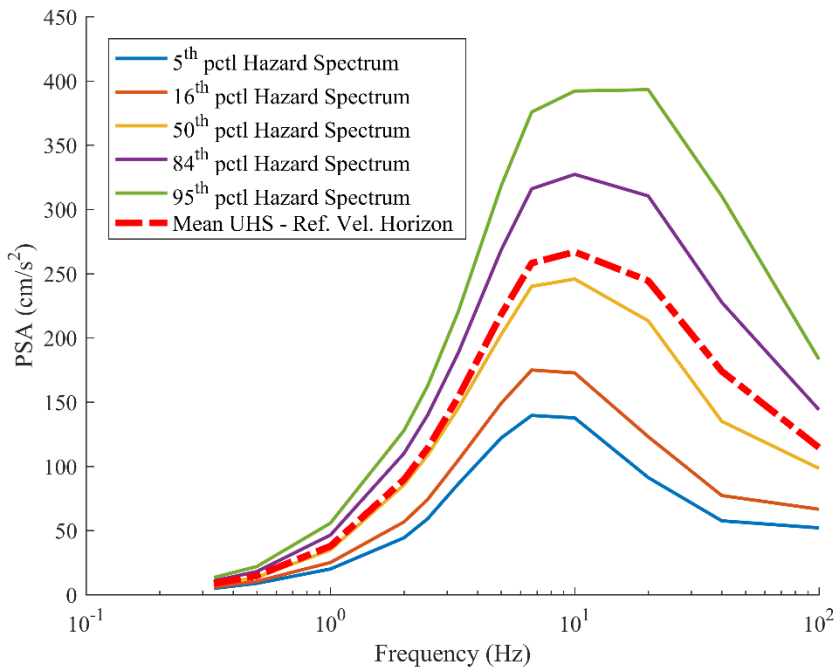
642 Hazard results were calculated for selected percentiles ranging from the 5<sup>th</sup> to the 95<sup>th</sup>, in  
643 addition to the mean estimates. Hazard estimates were calculated for a total of 12 spectral  
644 ordinates [i.e., PGA and 5% damped pseudo-spectral accelerations (PSA) at 0.025, 0.05,  
645 0.10, 0.15, 0.20, 0.30, 0.40, 0.50, 1.00, 2.00 and 3.00 s]. Hazard results at the reference  
646 velocity horizon were provided in terms of hazard curves, and uniform hazard spectra (UHS),

647 disaggregated results, controlling earthquake scenarios and scenario spectra for selected  
648 return periods.

649 Disaggregated results were only provided for PGA and PSA at 0.1, 0.2, 0.4 and 1.0 s.  
650 Disaggregated results for PGA were provided as it is common practice to provide a full set of  
651 results for this parameter. Disaggregated results for the remaining oscillator periods were  
652 relevant for the derivation of disaggregated results representative of the high-frequency (HF;  
653 5 to 10 Hz) and low-frequency (LF; 1 to 2.5 Hz) ranges in accordance with the U.S. NRC  
654 Regulatory Guideline 1.208 (USNRC 2007). HF and LF range disaggregated results were  
655 then used to define the controlling scenarios for the development of the scenario spectra to be  
656 used in the site-response analysis.

## 657 5.2. Hazard Results at Reference Velocity Horizon

658 The mean UHS and response spectra for selected percentiles, for the reference velocity  
659 horizon, corresponding to the design return period of 10,000 years (annual frequency of  
660 exceedance, AFoE, of  $10^{-4}$ ) are presented in Figure 11.



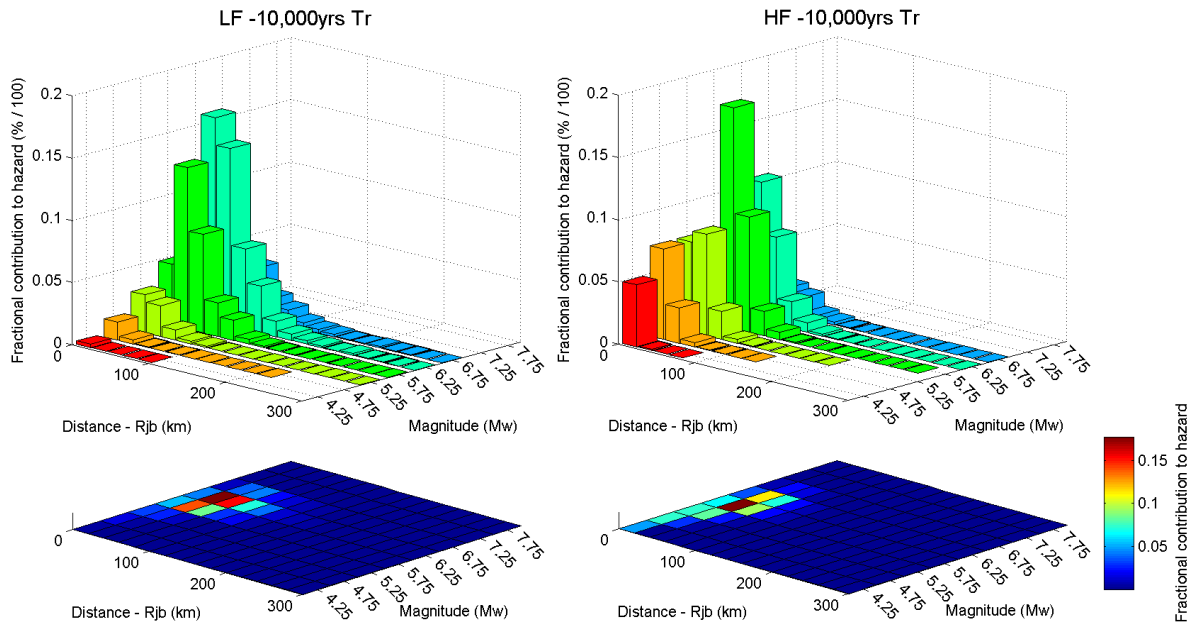
661  
662 **Fig. 11**  $10^{-4}$  AFoE mean UHS and hazard spectra for selected percentiles for the reference velocity  
663 horizon

664 Disaggregated results in terms of magnitude and distance were produced for AFoEs  
665 ranging from  $10^{-3}$  to  $10^{-6}$  for the LF and HF ranges in order to estimate the controlling  
666 scenarios to be used as input for the derivation of the scenario spectra required for the site-

667 response analysis. LF- and HF-range disaggregated results for the AFoE of  $10^{-4}$  are presented  
 668 in Figure 12 in terms of magnitude and distance.

669 In addition to the controlling scenarios for the LF and HF ranges, USNRC (2007)  
 670 recommends that for the LF range, when contributions to the hazard from events with  
 671 distances  $\geq 100$  km are equal to or exceed 5% of the total hazard, controlling scenarios  
 672 considering only contributions from events in that range of distances should be assessed. This  
 673 condition was met only in the disaggregated results for the AFoE of  $10^{-3}$ . A summary of the  
 674 controlling scenarios in terms of magnitude and distance is presented in Table 1.

675 Unscaled scenario spectra to be used as input to the site-response analysis were derived  
 676 for each of the controlling scenarios presented in Table 1. The scenario spectra were obtained  
 677 as the weighted mean of the median response spectra obtained for each of the GMPEs,  
 678 including their alternative  $V_S$ -kappa adjustment factors, in the ground-motion logic tree.



679  
 680 **Fig. 12** Disaggregated results by magnitude-distance bins with an AFoE of  $10^{-4}$  for the low-frequency  
 681 (LF) range (left) and the high-frequency (HF) range (right)

682 **Table 1** Controlling earthquake scenarios for the various AFoE of interest, for the high-frequency  
 683 (HF), low-frequency (LF) ranges, and for the low-frequency range considering events with distances  
 684  $\geq 100$ km (LF100) when the contributions from that range of distances is equal to or greater than 5%  
 685 (%LF100)

AFoE \ Range	$10^{-3}$		$10^{-4}$		$10^{-5}$		$10^{-6}$	
	$M_w$	$R_{jb}$	$M_w$	$R_{jb}$	$M_w$	$R_{jb}$	$M_w$	$R_{jb}$
<b>HF</b>	5.50	43.9	5.66	31.4	5.75	21.8	5.82	14.7

<b>LF</b>	5.83	65.6	6.06	45.8	6.17	31.5	6.24	20.3
<b>LF100</b>	6.16	153.6	N/A		N/A		N/A	
<b>%LF100</b>	14		4		1		0.3	

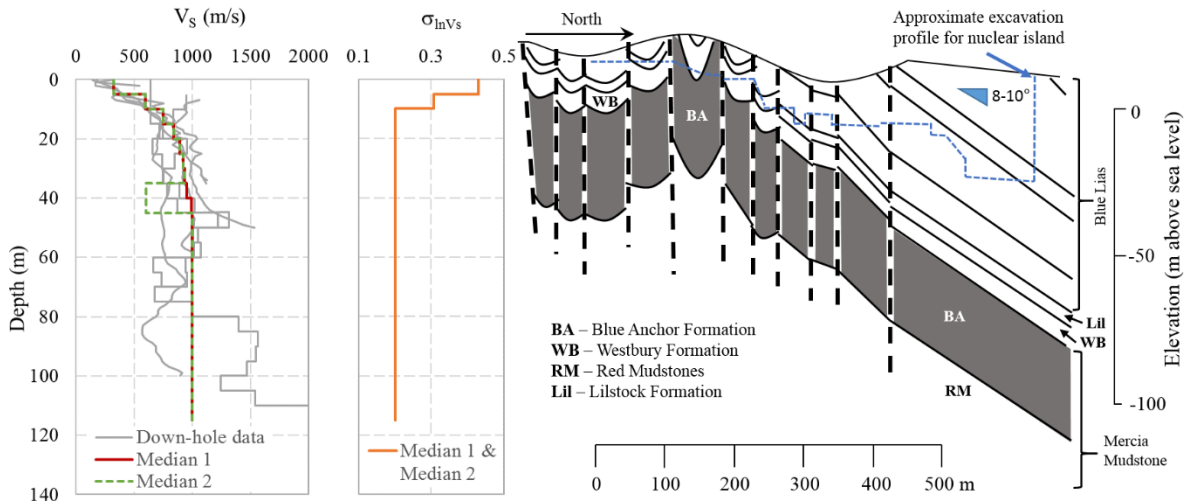
686

687 **6. Site Characterization**

688 The geological characterization of the site required a large body of ground investigation  
689 reports to be reviewed for the existing and newly proposed NPPs at Hinkley Point,  
690 undertaken between the late 1960s and 2010. In addition to the historical campaigns, two  
691 single-station microtremor surveys were conducted in 2014 and 2015 as part of the Hinkley  
692 PSHA (BRGM 2014, 2015).

693 The site characterization focused on the soil and rock parameters required for the site  
694 response analysis, namely: shear-wave velocity,  $V_S$  and its variation with depth; dependency  
695 of the shear modulus,  $G$ , and damping ratio,  $D$ , on shear strain,  $\gamma_s$  for each individual  
696 geological unit, and saturated density,  $\rho_{sat}$ , for the different geological units. Separate  
697 assessments were made for the onshore and offshore domains of the site, although the current  
698 article focuses only on the onshore characterization. A more detailed description of the  
699 derivation of the dynamic soil and rock properties is presented in the companion paper by  
700 Lessi-Cheimariou et al. (2018).

701 The variation of  $V_S$  with depth was defined following a detailed review of data from the  
702 historical ground investigations and geophysical surveys. Significant differences were  
703 identified between  $V_S$  values from the cross-hole and down-hole techniques. The results from  
704 the cross-hole testing were strongly influenced by the presence of stiff limestone bands  
705 within the parent mudrock which caused an overestimation of  $V_S$  in the mudrock due to  
706 refraction of the seismic waves along the stiffer layers. More credence was ultimately given  
707 to the shear-wave velocities from the down-hole tests, resulting in the definition of the  
708 “Median 1”  $V_S$  profile and the corresponding variability,  $\sigma_{lnV_S}$ , shown in Figure 13.



709

710 **Fig. 13** Onshore model comprising two median  $V_S$  profiles, the proposed variability of the natural  
 711 logarithm of the  $V_S$  ( $\sigma_{\ln V_S}$ ) and the down-hole data used to derive the model. The shear-wave velocity  
 712 reversal in Median 2 (green dashed line) at 35 m corresponds to the Westbury Formation (WB) in the  
 713 central part of the site. Principal geological strata are shown in a typical north-south cross-section  
 714 through the proposed nuclear island. The reference velocity horizon was defined at the top of the Blue  
 715 Anchor Formation (BA)

716 The interpretation of the data from the two recent microtremor campaigns (BRGM 2014,  
 717 2015) consistently showed the presence of a 3.5 Hz peak in the horizontal-to-vertical spectral  
 718 ratio for locations in the northern part of the site. Site response sensitivity analyses  
 719 demonstrated that this characteristic peak was most likely associated with the presence of a  
 720 shear-wave velocity reversal related to the Westbury Formation, which is encountered in this  
 721 area of the site between about 35 m and 45 m depth. It was considered important to capture  
 722 this feature in the site response analysis through the definition of a second  $V_S$  profile,  
 723 “Median 2”, as shown in Figure 13. The same  $\sigma_{\ln V_S}$  established for Median 1 was used for  
 724 Median 2.

725 As highlighted in the cross-section in Figure 13, the strata underlying the HPC site are  
 726 dipping gently 8 to 10 degrees northwards. This presented a challenge for definition of a  
 727 suitable reference velocity horizon, as the depth to any single geological unit varies from  
 728 south to north across the nuclear island by approximately 70 m. On reviewing the strata  
 729 present on site, the Blue Anchor Formation appeared to be the best candidate for the  
 730 reference velocity horizon, based on the range of measured  $V_S$  within that unit, with a median  
 731 shear-wave velocity of 1,000 m/s, and the need for the reference velocity horizon to be  
 732 beneath the Westbury Formation, whose significance was highlighted by the microtremor  
 733 investigation. The site response approach accounted for the variability in the range of

734 measured  $V_S$  and the depth to the reference velocity horizon, as explained in the following  
735 section.

736 Due to a lack of reliable site-specific cyclic tests, non-linear properties of the mudstones  
737 were based on the earlier work of Nuclear Electric (NE 1995), also presented in Davis et al.  
738 (1996). They reinterpreted shear modulus degradation and damping curves from cyclic  
739 laboratory testing of soft rocks from other sites (Hara and Koyota 1977; Nishi et al. 1983; and  
740 Kim 1992) in the light of non-linear properties from monotonic in situ and laboratory testing  
741 of samples of mudstone from HPC. A distinction was made in the nonlinear properties  
742 between the shallower strata ( $\leq 25$  m deep) and deeper strata ( $> 25$  m) in order to reflect the  
743 variations in lithology and the weathering of the rock at HPC.

## 744 **7. Site Response Analysis**

745 The site response analysis was performed as part of the partially non-ergodic PSHA to  
746 determine the median of the site term and its associated variability. The median site term,  
747 which expresses the average deviation of the ground motions at a site from the predictions of  
748 the GMPEs at the reference velocity horizon, can also be determined by statistical analysis of  
749 site-specific ground motions (Rodriguez-Marek et al. 2014), where suitable and sufficient  
750 records exist. Due to lack of site-specific records for the HPC site, the numerical site  
751 response approach, as described in the following sub-sections, was adopted for this study to  
752 estimate the site term. Separate analyses were performed for the onshore and offshore  
753 domains, although only results for the onshore domain are presented herein.

### 754 **7.1. Method of Analysis**

755 Site response analyses were performed in accordance with the recommendations of the  
756 USNRC Regulatory Guidelines (USNRC 2007) and the requirements for a partially non-  
757 ergodic PSHA (Rodriguez-Marek et al. 2014) using the software STRATA (Kottke et al.  
758 2013). The analyses were performed using the best estimates of the site properties and  
759 incorporated the variability in the various site properties using Monte Carlo simulations and  
760 the following statistical models, which are integrated into STRATA (Kottke et al. 2013):

- 761 • The shear-wave velocity was varied based on the median  $V_S$  profile and the  $\sigma_{\ln V_S}$  using  
762 the Toro (1995) model. The principal assumption of the Toro (1995) model is that the  
763 shear-wave velocities are characterized by a log-normal distribution. Upper and lower  
764 bounds of  $\pm 2.0 \sigma_{\ln V_S}$  around the median value were adopted to ensure that the realizations

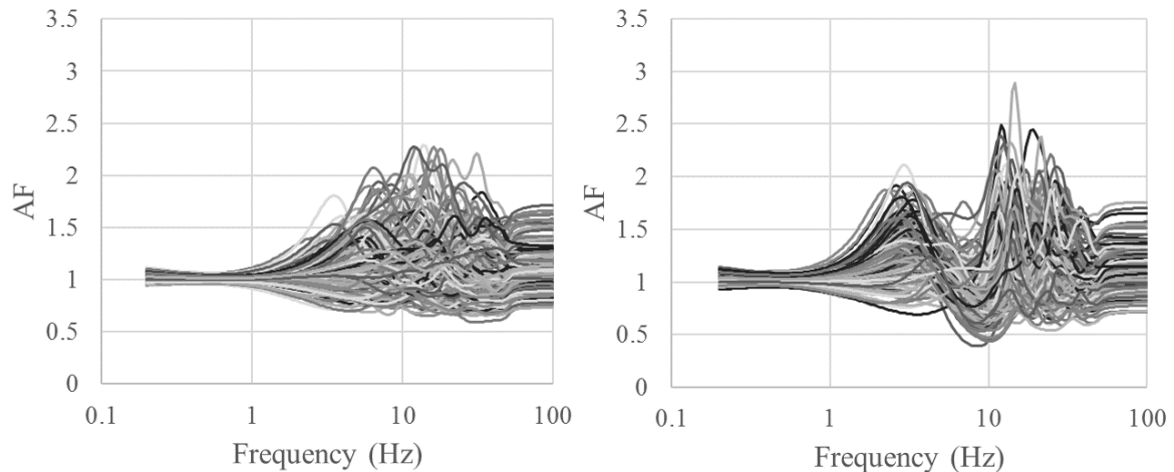
765 were not unrepresentative of the measured data and following the recommendations from  
766 EPRI (2013). The input and output  $\sigma_{InVs}$ , from a total of 1,000 Monte Carlo simulations,  
767 were compared to ensure that the input variability was preserved by the simulated shear-  
768 wave velocity profiles, a good agreement was achieved between the input and resulting  
769  $\sigma_{InVs}$ .

- 770 • The generic layering model after Toro (1995) was used for generating layering within the  
771 soil/rock column, assuming a non-homogeneous Poisson process where the number of  
772 layer interfaces per meter varies with depth.
- 773 • The nonlinear properties were varied using the Darendeli (2001) model which assumes  
774 that both the shear modulus reduction and damping curves are normally distributed. The  
775 shear modulus reduction and damping curves were correlated using a correlation  
776 coefficient equal to -0.5, implying that a value of shear modulus reduction above the  
777 mean (higher stiffness) will be related with lower damping.
- 778 • The depth to reference velocity horizon was modelled using a uniform distribution to  
779 capture the influence of the shallow northward dip of the geological bedding. This  
780 introduces an averaging effect of the site response across the nuclear island footprint,  
781 which is considered a desirable outcome as the nuclear island will be resting on a  
782 monolithic concrete raft.

783 The input motions were defined based on the approach in USNRC (2007). The selection  
784 of other input parameters was based on the results of parametric analyses and empirical  
785 relationships as described before.

786 Equivalent linear (EQL) random vibration theory (RVT) site response analysis was  
787 performed. The use of EQL site response analysis was justified (e.g., Kaklamanos et al. 2013;  
788 Stewart et al. 2014) by the low strain response ( $\sim < 0.1\%$ ). It was also demonstrated that RVT  
789 site response analysis did not introduce a systematic bias in comparison to time-series site  
790 response analysis (Bard et al. 2004; Kottke and Rathje 2013; Lessi-Cheimariou et al. 2018)  
791 due to the site response concentrated at high frequencies. RVT site response analysis was  
792 preferred due to its computational efficiency and because input motion acceleration time  
793 histories do not need to be defined and selected. A total of 1,000 Monte Carlo simulations  
794 were performed for each scenario spectrum and median  $V_S$  profile considered. Amplification  
795 factors (AFs) of a representative subset of these 1,000 simulations, for the high-frequency  
796 scenario spectrum,  $10^{-4}$  AFoE, and for both Median 1 and Median 2  $V_S$  profiles, are shown in

797 Figure 14. It is noted that all site response analysis outputs were computed for a target  
798 velocity horizon (i.e. target foundation level) of 5 m below existing ground level, recognizing  
799 that the shallowest material will be removed during the construction. The  $V_{S30}$  representative  
800 of the target velocity horizon is 802 m/s.



801

802 **Fig. 14** Amplification factors for Median 1 (left) and Median 2 (right), high-frequency scenario  
803 spectrum, AFoE  $10^{-4}$

804 The results from the site response analysis were integrated with the hazard estimates at  
805 the reference velocity horizon using Convolution-Approach 3 (McGuire et al. 2001; Bazzurro  
806 and Cornell 2004), which have the advantage of computational and project organizational  
807 efficiency of treating the site response analysis as a post-processing step in the computations,  
808 thus decoupling the site response analysis from the bedrock hazard calculations.

809 A logic tree was developed to capture the epistemic uncertainty associated with the  
810 determination of the  $V_S$  model. A higher weight,  $2/3$ , was assigned to Median 1 to reflect the  
811 fact that it was representative of the conditions across the entire site whilst a weight of  $1/3$   
812 was assigned to Median 2 which was only representative of the ground conditions to the  
813 north of the site where the microtremor results indicated a characteristic 3.5 Hz peak. An  
814 additional level of branches for analysis with and without Monte Carlo simulations was  
815 proposed to address the issue of potential over-smoothing of the amplification factors, which  
816 can occur when Monte Carlo simulations are performed (Bard et al. 2004). Equal weights  
817 were assigned to these branches as there was no justification to give more credence to either  
818 type of analysis. In order to be able to implement the convolution approach for the analyses  
819 without any Monte Carlo simulations, the standard deviation was adopted from the  
820 corresponding analyses which included Monte Carlo simulations.

821 Seismic hazard curves for the 5<sup>th</sup>, 16<sup>th</sup>, 50<sup>th</sup>, 84<sup>th</sup> and 95<sup>th</sup> percentiles were calculated for  
822 the target horizon level using the approach recommended in EPRI (2013). This approach  
823 involves combining the site response logic-tree branches into a single composite distribution  
824 of logarithmic amplification factors (lnAF), with equivalent mean and variance, and is  
825 justified by the fact that all individual branch tips of the site response logic-tree are normal  
826 distributions of lnAF. An alternative implementation involving convolution of the reference  
827 horizon hazard with the individual site response logic-tree branches, and then recombining  
828 surface hazard branches was also explored, but found to be less robust numerically. In the  
829 particular case of HPC, the lnAF distribution shows very little departure from linearity, so the  
830 convolution with the combined lnAF distribution preserves the reference horizon percentiles  
831 as it is a monotonically increasing transformation (Pearson & Tukey, 1965).

## 832 **7.2. Epistemic Uncertainty of the Site Term and $\delta\phi_{S2S}$**

833 An assessment was carried out to ascertain whether the proposed site response model  
834 adequately captured the epistemic uncertainty of the AFs across the full range of response  
835 periods. From that assessment, it was considered necessary to apply correction factors to the  
836 computed values of  $\sigma_{\ln AF}$  (standard deviation of the natural logarithm of the amplification  
837 factor from the site response analyses) at the longer periods, where this quantity was not well  
838 resolved owing to the onset of bandwidth limitation in the site response approach. This  
839 correction was applied to ensure a minimum floor level, equal to 0.1 natural logarithm units,  
840 for the logic-tree branches including Monte Carlo randomizations. For the branches without  
841 Monte Carlo randomizations, the  $\sigma_{\ln AF}$  values of the equivalent Monte Carlo branches were  
842 adopted, since the principal purpose of removing the randomizations was to ensure that the  
843 median behavior was adequately captured and, therefore, did not impose constraints on the  
844 definition of the variability. Sensitivity analyses showed that the choice of the floor level  
845 value (within reasonable limits) had little impact on the surface hazard results, and thus the  
846 selected value of 0.1 was considered appropriate for all branches of the site response logic-  
847 tree.

## 848 **8. Seismic Hazard at Target Horizon**

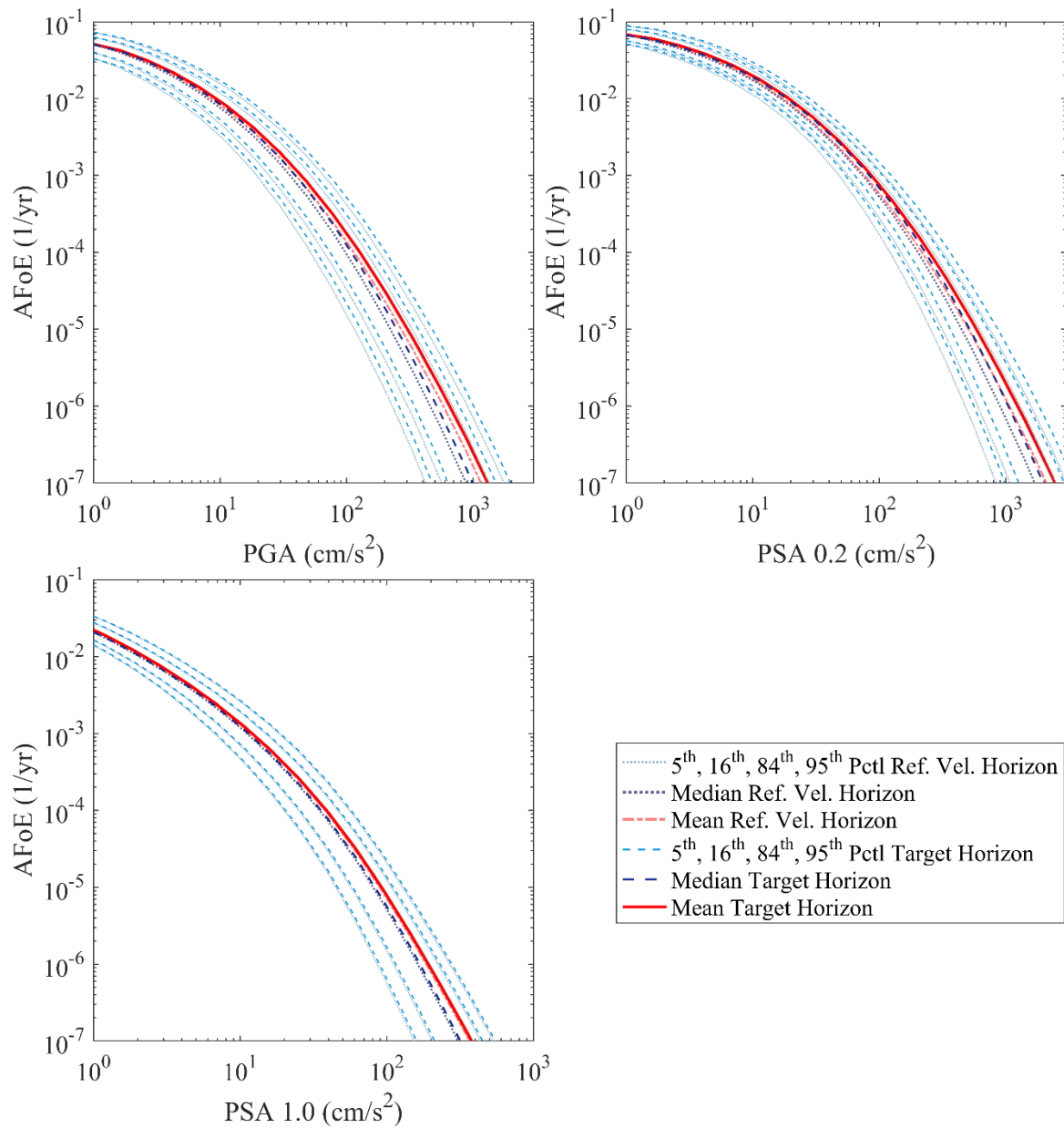
849 Seismic hazard estimates at the target horizon (i.e., target foundation level) were provided  
850 in the form of hazard curves for the mean and the 5<sup>th</sup>, 16<sup>th</sup>, 50<sup>th</sup>, 84<sup>th</sup> and 95<sup>th</sup> percentiles for  
851 the 12 response periods of interest. In addition to this, mean UHS and response spectra for the  
852 selected percentiles were derived for a range of AFoE between  $10^{-3}$  and  $10^{-6}$ .

853 **8.1. Onshore Results**

854 Figure 15 presents a comparison of the PGA, PSA(0.2s) and PSA(1.0s) mean hazard  
855 curves for the target horizon and the reference velocity horizon along with hazard curves at  
856 target horizon for selected percentiles [i.e., 5th, 16th, 50th (median), 84th and 95th].

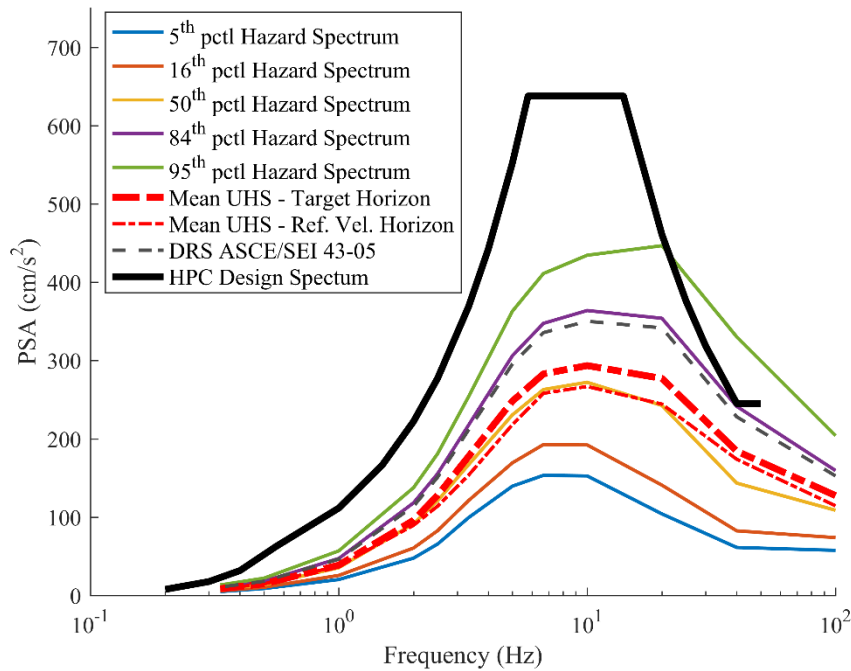
857 Figure 16 compares the  $10^{-4}$  AFoE UHS and response spectra for the 5<sup>th</sup>, 16<sup>th</sup>, 50<sup>th</sup>, 84<sup>th</sup>  
858 and 95<sup>th</sup> percentiles at target horizon against the HPC design spectrum. From this  
859 comparison, it is clear that the HPC design basis spectrum comfortably envelopes the 84<sup>th</sup>  
860 percentile response spectra at the target horizon across the whole range of frequencies, with  
861 the exception of PSA at 40 Hz where the HPC design basis spectrum is only slightly higher  
862 than the 84<sup>th</sup> percentile spectrum.

863 In the UK regulatory context, the design basis spectrum, commonly pre-defined at an  
864 early stage as part of the generic design assessment, is expected to envelope the 84<sup>th</sup>  
865 percentile response spectra with an AFoE of  $10^{-4}$  obtained from a site-specific PSHA. This is  
866 somewhat different to the approach in the US for the seismic design of nuclear facilities  
867 (ASCE/SEI 43-05), where the design response spectrum (DRS) for structures with seismic  
868 design category 5 (e.g., the nuclear island in a NPP would be classified as SDC-5) is obtained  
869 from the multiplication of the  $10^{-4}$  AFoE UHS and a ‘design factor’ which is dependent on  
870 the slope of the seismic hazard curve for the target foundation level, of each response period  
871 available in the UHS, at around an AFoE of  $10^{-4}$ . For the particular case of the HPC site, the  
872  $10^{-4}$  84<sup>th</sup> percentile response spectrum is slightly more conservative than the DRS derived in  
873 accordance with ASCE/SEI 43-05 (see Figure 16). However, this conclusion may not hold  
874 for other sites.



875

876 **Fig. 15** Mean and 5<sup>th</sup>, 16<sup>th</sup>, 50<sup>th</sup> (median), 84<sup>th</sup> and 95<sup>th</sup> percentile hazard curves for the onshore target  
 877 foundation level at the Hinkley Point site



878

879 **Fig. 16**  $10^{-4}$  AFoE mean UHS at target and reference velocity horizons, and  $10^{-4}$  AFoE hazard spectra  
 880 for selected percentiles at target horizon, compared against the HPC design spectrum

881 From Figure 16, it can also be observed that the level of ‘conservatism’ of the design  
 882 basis spectrum is not uniform across the full range of frequencies of interest, with lower  
 883 levels of conservatism at the high frequencies ( $> 20$  Hz). The main reason for this lower level  
 884 of conservatism in the HPC design basis spectrum is that it was derived using the piecewise  
 885 linear design response spectra defined in the European Utility Requirements for Light Water  
 886 Reactor Nuclear Power Plants (commonly referred as EUR spectra) whose origins date to the  
 887 1980s. The EUR spectra, therefore, do not incorporate recent developments in the  
 888 understanding of the characterization of ground motion, which affects particularly the high  
 889 frequency range of the spectrum. Similar observations have been made at other similar sites  
 890 in the UK and the US. A more detailed discussion on the EUR spectrum is provided by  
 891 Bommer et al. (2011) and Coatsworth (2015).

892 **9. Assessing Epistemic Uncertainty**

893 In PSHA the spread of the percentiles calculated using the full set of hazard curves from  
 894 the logic tree represents the epistemic uncertainty in the results. The greater the spread of the  
 895 percentiles, the higher the epistemic uncertainty. Assessing whether the level of epistemic  
 896 uncertainty captured by the logic tree of a particular PSHA is adequate for the level and  
 897 objectives of the study is not a trivial task as it implies quantification of the “unknown”. To  
 898 do this, first a metric to “measure” in a consistent manner the level of uncertainty captured in

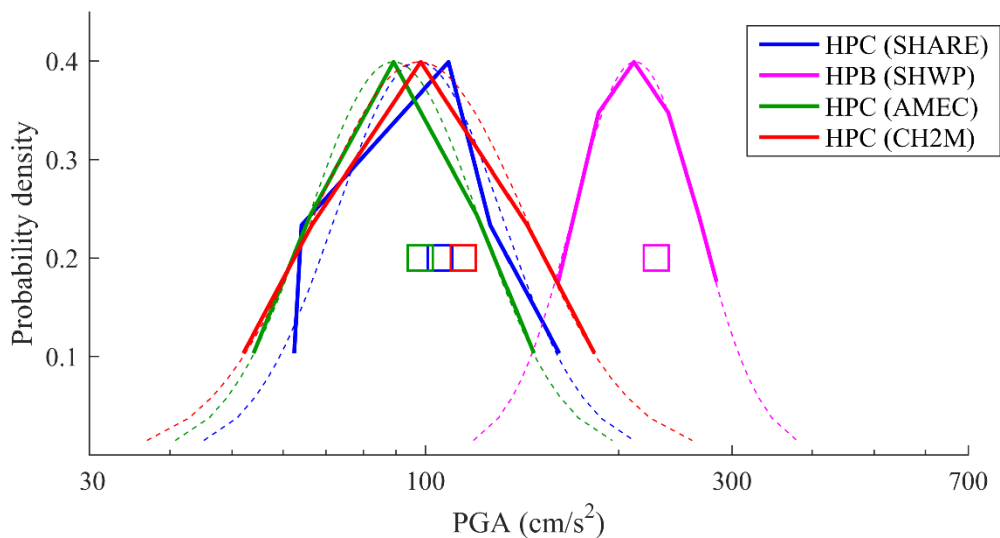
899 a PSHA needs to be specified; secondly, a criterion defining acceptable levels of epistemic  
900 uncertainty needs to be defined depending on the level of rigour and objectives of the PSHA  
901 study. Various metrics to measure the epistemic uncertainty captured in a PSHA are  
902 discussed by Douglas et al. (2014). However, to the knowledge of the authors of this paper,  
903 no criterion to define minimum acceptable levels of epistemic uncertainty in a PSHA has  
904 been proposed and developing a criterion may not even be possible due to the intrinsic  
905 “unknown” nature of epistemic uncertainty as discussed above. It should be noted that  
906 minimum levels of epistemic uncertainty associated with specific elements of the PSHA can  
907 be defined based on amount and quality of data available (e.g. EPRI 2013); however, the  
908 discussion presented in this section concerns the “overall” epistemic uncertainty captured by  
909 the PSHA study.

910 More rigorous PSHA studies, such as those related to the safety of nuclear facilities  
911 (equivalent to SSHAC Level 3 or 4), are expected to better capture the full range, body and  
912 center of the epistemic uncertainty than less rigorous PSHA studies, common for the design  
913 of conventional structures (equivalent to SSHAC Level 1 or 2), as more time and effort has  
914 been spent on constraining the ‘unknowns’. More rigorous studies, by virtue of their greater  
915 investment in data collection, may allow a genuine reduction in epistemic uncertainty, which  
916 is in contrast to the apparently low (but actually underestimated) uncertainties shown by a  
917 narrow spread in hazard curves in less rigorous studies (e.g. Douglas et al., 2014).

918 A way to assess whether epistemic uncertainty has been adequately captured in a PSHA is  
919 through historical precedent, by comparing the distribution of selected percentiles at a given  
920 return period from the PSHA of interest against other PSHA studies with similar level of  
921 rigour and levels of seismic activity. Douglas et al. (2014) present a comparison of results  
922 from various published PSHA reporting mean, median and 16<sup>th</sup> (or 15<sup>th</sup>) and 84<sup>th</sup> (or 85<sup>th</sup>)  
923 percentiles for PGA for the 475- and 2,475-year return periods.

924 A similar approach to Douglas et al. (2014) was followed in this study, comparing the  
925 epistemic uncertainty captured in the Hinkley PSHA logic tree against data from previous  
926 studies providing hazard estimates for the Hinkley site [i.e., SHWP 1987; AMEC 2012; and  
927 Woessner et al. 2015 (SHARE Project)]. For each of these projects, empirical probability  
928 distribution functions (PDFs) were derived using the available percentiles, for AFoEs of  $10^{-4}$   
929 and  $10^{-5}$ , for PGA and PSA at 0.2 s and 1.0 s. Figure 17 presents the comparison of the  
930 empirical PDFs (solid lines), and best fit to the log-normal distributions of the various  
931 percentiles (dashed lines), for PGA with an AFoE of  $10^{-4}$ . Similar results were observed for

932 an AFoE of  $10^{-5}$  and for PSA at 0.2 s and 1.0 s; figures for these parameters and AFoE are not  
 933 presented here because of space limitations.



934  
 935 **Fig. 17** Probability density functions derived from percentiles for PGA from various projects and for  
 936 the Hinkley PSHA. Solid lines are empirical PDFs based on the percentiles available for each study;  
 937 dashed lines are the best fit to the log-normal distribution of the percentiles; squares indicate the  
 938 means

939 The SHWP (1987) study was the first of a series of site-specific studies undertaken for  
 940 UK nuclear power plant sites in the late 1980s, early 1990s, which were considered state-of-  
 941 the-art at the time and incorporated epistemic uncertainty through the use of the logic tree  
 942 framework. However, one of the main limitations of the SHWP (1987) study, when compared  
 943 to modern practice, is the use of single GMPE for the hazard evaluation. This is likely to be  
 944 the reason for the much smaller spread in the SHWP results than the other studies, as the  
 945 selection of the suite of GMPEs to be used in the hazard assessment has been found to be the  
 946 largest contributor to epistemic uncertainty in PSHA (e.g., Stepp et al. 2001).

947 The AMEC (2012) study was carried out as a site-specific study for the HPC site with a  
 948 more limited scope than the study presented in this paper, equivalent to a SSHAC Level 1  
 949 study, which was aimed at providing an early indication of the seismic hazard levels at the  
 950 HPC site using more modern methods than the SHWP study, particularly regarding the use of  
 951 modern GMPEs. The SHARE study, based on a European project aimed at providing a Euro-  
 952 Mediterranean seismic hazard model and to establish new standards in PSHA practice, is the  
 953 only non-site-specific study included here. Hazard results from the SHARE project for a  
 954 specific location within the project area are available from their web page  
 955 (<http://www.efehr.org/en/home/>).

956 The PDFs of the assessed ground motions from the independent studies by SHARE,  
957 AMEC and CH2M (this study) show considerable overlap. This lends confidence that the  
958 results obtained for the Hinkley PSHA are a good representation of the seismic hazard at this  
959 site and that the uncertainties have been appropriately captured. Although the results from the  
960 CH2M, AMEC and SHARE studies show similar levels of epistemic uncertainty, a higher  
961 level of confidence is associated with CH2M's empirical PDF due to the site-specific nature  
962 of the study, as opposed to the regional nature of the SHARE project and to the greater level  
963 of effort and rigour/formalism of CH2M's PSHA process compared to that of the AMEC  
964 study. The relation between the level of rigour and objectives of a study, and the level of  
965 confidence in their results is clearly summarized by Budnitz et al. (1997): "*there is nothing*  
966 *inherently 'wrong' with the calculated results that come from a modest hazard analysis*  
967 *conducted by a single contractor; nor does the use of multiple experts in a large-scale project*  
968 *guarantee that the hazard results are more defensible (particularly if done poorly). They are,*  
969 *however, more likely to capture accurately the scientific community's information"*.

## 970 **10. Conclusions**

971 A state-of-the-art PSHA has been carried out for the HPC site with the objective of  
972 underpinning the HPC design basis spectrum and providing input to inform the probabilistic  
973 safety assessment elements for the Safety Case. This is the first time that a seismic hazard  
974 study for a NPP in the UK has successfully passed through the regulatory approval process  
975 since the work done by the SHWP in the 1980s and early 1990s for the existing fleet of UK  
976 nuclear power stations. The present study is consistent with international best practice and  
977 incorporated a number of key elements, summarised below.

978 A project-specific earthquake catalogue was developed, including archive search to  
979 collect data on known events and to identify previously undiscovered earthquakes. The  
980 seismicity model considered fourteen seismic sources, combined to form six alternative  
981 seismic source models in order to capture the main sources of epistemic uncertainty  
982 associated with the delineation of the source boundaries, and in particular with the location of  
983 the Variscan Front which demarcates the boundary between the higher levels of seismicity in  
984 South Wales and the lower levels observed south of the Bristol Channel.

985 Recurrence rates were determined for all the seismic source zones considering the  
986 doubly-truncated exponential Gutenberg-Richter model. To capture the epistemic  
987 uncertainties associated with earthquake recurrence, nine alternative combinations of the

988 activity (a) rate and b-value parameters were defined for the host seismic source and the next  
989 two most hazard-significant seismic sources. Logic tree weights were source-specific as they  
990 were based on a maximum-likelihood fit to the data.

991 The ground-motion model was developed using separate models for the median ground-  
992 motion and aleatory variability. The median ground-motion model comprised a suite of five  
993 GMPEs adjusted to the site-specific conditions using  $V_S$ -kappa factors. A partially non-  
994 ergodic sigma model was adopted with separate components for the inter-event variability,  
995 and single-station intra-event variability, adjusted by a partially ergodic site-to-site variability  
996 term.

997 Site response analysis was performed using equivalent-linear random vibration theory  
998 with explicit incorporation of the variability in the ground properties using Monte Carlo  
999 simulations. The final PSHA results were obtained by convolution of the hazard at the  
1000 reference rock horizon with the site amplification factors. The HPC design basis spectrum  
1001 was shown to envelope the 84th percentile UHS across all frequencies with the exception of  
1002 PSA at 40 Hz, where a marginal exceedance was observed.

1003 The overall epistemic uncertainty captured by the logic tree was assessed and compared  
1004 against results from earlier PSHA studies for the same site. The epistemic uncertainty was  
1005 similar amongst all studies, except for SHWP (1987) which showed a lower level of  
1006 epistemic uncertainty, attributed mainly to the use of a single GMPE in their study. Despite  
1007 the similar levels of epistemic uncertainty captured by the most recent studies, a higher level  
1008 of confidence is associated with the empirical PDF from the current study due to the greater  
1009 level of effort on constraining the epistemic uncertainty and the greater rigour of the PSHA  
1010 process.

## 1011 **11. Acknowledgments**

1012 The authors of this paper would like to thank the participation of all members of the  
1013 Technical Delivery Team who take full intellectual ownership of the models, and logic trees,  
1014 developed as part of the Hinkley PSHA. The authors would like to thank as well the various  
1015 Subject Experts that were interviewed as part of the project: Dr Tim Pharaoh, Nigel Smith,  
1016 Dr Andy Chadwick, Dr Alastair Ruffell, Prof. Andreas Rietbrock, Dr Peter Stafford, Prof.  
1017 Fabrice Cotton, Prof. Ellen Rathje, Prof. Pierre-Yves Bard, Dr-Ing Philippe Renault, Dr Rod  
1018 Graham and Prof. Dave Sanderson. The TDT is certainly in debt to the Peer-Review team, Dr  
1019 Hilmar Bungum and Dr Martin Koller, for their constructive, challenging and insightful

1020 review of all deliverables of the project. Our thanks go as well to the dedicated Project  
1021 Management team, Guy Green and Liz Rivers, for their continued efforts to keep the TDT  
1022 within budget and on schedule, to the GEM Foundation for their collaboration on the cross-  
1023 checking calculations, and to Prof. Mario Ordaz for providing CRISIS2015 and responding to  
1024 our queries on the use of the software. The authors would also like to thank the two  
1025 anonymous reviewers for their valuable comments.

1026 Contributions from William Aspinall, who kindly provided the data from the Hinkley  
1027 Point microseismic array installed and operated by the Seismic Hazard Working Party in the  
1028 1980s and early 1990s, and from the British Geological Survey, who provided ground-motion  
1029 records for the UK, are acknowledged. Finally, we express our gratitude to NNB GenCo, the  
1030 sponsor of the project, for agreeing to the publication of this paper.

## 1031 **12. References**

- 1032 Abrahamson N A, Silva W J, Kamai R (2014) Summary of the ASK14 ground-motion  
1033 relation for active crustal regions. *Earthq Spectra* 30 (3):1025-1055
- 1034 Al Atik L (2014) Candidate ground motion models and logic-tree structure for sigma: models  
1035 for tau. Presentation at SWUS GMC SSHAC Level 3 Workshop 3, December 4
- 1036 Al Atik L, Kottke A, Abrahamson N, Hollenback J (2014) Kappa ( $\kappa$ ) scaling of ground-  
1037 motion prediction equations using an inverse random vibration theory approach. *Bull Seismol*  
1038 *Soc Am* 104 (1):336-346
- 1039 Aldama-Bustos G, Tromans I J, Strasser F, Garrard G, Green G, Rivers L, Douglas J, Musson  
1040 R M W, Hunt S, Lessi-Cheimariou A, Daví M, Robertson C (2018) A streamlined approach  
1041 for the seismic hazard assessment of a new nuclear power plant in the UK. *Bull Earthquake*  
1042 *Eng*, submitted
- 1043 AMEC (2012) UK EPR Project probabilistic seismic hazard assessment for Hinkley Point  
1044 Site C. Report number 15118/TR/0019, Rev. F BPE, NNB GenCo / AMEC Geomatrix, 364  
1045 pgs
- 1046 ASCE/SEI 43-05 (2005) Seismic design criteria for structures, systems, and components in  
1047 nuclear facilities. American Society of Civil Engineers / Structural Engineering Institute.
- 1048 Atkinson G M, Boore D M (2006) Earthquake ground motion prediction equations for eastern  
1049 North America. *Bull Seismol Soc Am* 96 (6):2181-2205
- 1050 Atkinson G M, Boore D M (2011) Modifications to existing ground-motion prediction  
1051 equations in light of new data. *Bull Seismol Soc Am* 10 (3):1121-1135
- 1052 Atkinson G M, Bommer J J, Abrahamson N A (2014) Alternative approaches to modeling  
1053 epistemic uncertainty in ground motions in probabilistic seismic-hazard analysis. *Seismol*  
1054 *Res Lett* 85 (6):1-4
- 1055 Bard P-Y (2008) Foreword - The H/V technique: capabilities and limitations based on the  
1056 results of the SESAME project. *Bull Earthquake Eng* 6 (1):1-2

1057 Bard P-Y, Fäh D, Pecker A, Studer J A (2004) Probabilistic seismic hazard analysis for Swiss  
1058 nuclear power plant sites (PEGASOS project): Elicitation summaries, Site response  
1059 characterisation (SP3). Final report Volume 6, Nationale Genossenschaft für die Lagerung  
1060 radioaktiver Abfälle (Nagra), 367 pgs

1061 Basili R, Kastelic V, Demircioglu M B, Garcia Moreno D, Nesmer E S, Petricca P, Sboras S  
1062 P, Besana-Ostman G M, Cabral J, Camelbeek T, Caputo R (2013) The European Database of  
1063 Seismogenic Faults (EDSF) compiled in the framework of the Project SHARE. Seismic  
1064 Hazard Harmonization in Europe, Seventh Framework Programme (FP7),  
1065 <http://diss.rm.ingv.it/share-edsf/>

1066 Bazzurro P, Cornell C A (2004) Nonlinear soil-site effects in probabilistic seismic-hazard  
1067 analysis. *Bull Seismol Soc Am* 94 (6):2110-2123

1068 BERR (2007) Meeting the energy challenge: A White Paper on nuclear power. CM 7296,  
1069 Department for Business Enterprise and Regulatory Reform, 192 pgs,  
1070 <https://www.gov.uk/government/publications/long-term-nuclear-energy-strategy>

1071 Bindi D, Massa M, Luzi L, Ameri G, Pacor F, Puglia R, Augliera P (2014a) Pan-European  
1072 ground-motion prediction equations for the average horizontal component of PGA, PGV, and  
1073 5%-damped PSA at spectral periods up to 3.0s using the RESORCE dataset. *Bull Earthquake*  
1074 *Eng* 12 (1):391-430

1075 Bindi D, Massa M, Luzi L, Ameri G, Pacor F, Puglia R, Augliera P (2014b) Erratum to: Pan-  
1076 European ground-motion prediction equations for the average horizontal component of PGA,  
1077 PGV, and 5%-damped PSA at spectral periods up to 3.0s using the RESORCE dataset. *Bull*  
1078 *Earthquake Eng* 12 (1):431-448

1079 Biro Y, Renault P (2012) Importance and impact of host-to-target conversions in PSHA.  
1080 Proceedings of the Fifteenth World Conference on Earthquake Engineering. Lisbon, Portugal.  
1081 Paper no. 1855

1082 Bommer J J (2012) Challenges of building logic trees for probabilistic seismic hazard  
1083 analysis. *Earthq Spectra* 28 (4):1723-1735

1084 Bommer J J, Crowley H (2017) The purpose and definition of the minimum magnitude limit  
1085 in PSHA calculations. *Seismol Res Lett* 88 (4):1097-1106

1086 Bommer J, Strasser F O, Pagani M, Monelli D (2013) Quality assurance for Logic-Tree  
1087 implementation in probabilistic seismic hazard analysis for nuclear applications: A practical  
1088 example. *Seismol Res Lett* 84 (6):938-945

1089 Bommer J J, Douglas J, Scherbaum F, Cotton F, Bungum H, Fäh D (2010) On the selection  
1090 of ground-motion prediction equations for seismic hazard analysis. *Seismol Res Lett* 81  
1091 (5):783-793

1092 Bommer J J, Papaspiliou M, Price W (2011) Earthquake response spectra for seismic design  
1093 of nuclear power plants in the UK. *Nuclear Engineering and Design* 241:968-977, doi:  
1094 10.1016/j.nucengdes.2011.01.029

1095 Bommer J J, Coppersmith K J, Coppersmith R T, Hanson K L, Mangongolo A, Neverling J,  
1096 Rathje E M, Rodriguez-Marek A, Scherbaum F, Shelembe R, Stafford P J, Strasser F O  
1097 (2015) A SSHAC Level 3 probabilistic seismic hazard analysis for a new-build nuclear site in  
1098 South Africa. *Earthq Spectra* 31 (2):661-698

- 1099 Boore D M, Stewart J P, Seyhan E, Atkinson G M (2014) NGA-West 2 equations for  
 1100 predicting PGA, PGV, and 5%-damped PSA for shallow crustal earthquakes. *Earthq Spectra*  
 1101 30 (3):1057-1085
- 1102 BRGM (2014) Microtremor survey conducted for Hinkley Point site (United Kingdom).  
 1103 BRGM/RC-64065-FR, Bureau de Recherches Géologiques et Minières, November 2014
- 1104 BRGM (2015) Supplementary microtremor survey conducted for Hinkley Point site (United  
 1105 Kingdom). BRGM/RC-64415-FR, Bureau de Recherches Géologiques et Minières
- 1106 Budnitz R J, Apostolakis G, Boore D M, Clu L S, Coppersmith K J, Cornell C A, Morris P A  
 1107 (1997) Recommendations for probabilistic seismic hazard analysis: Guidance on uncertainty  
 1108 and use of experts. NUREG/CR-6372: Vol. 1, US Nuclear Regulatory Commission, 280 pgs
- 1109 Burton P W, Musson R M W, Neilson G (1984) Studies of historical British earthquakes.  
 1110 Global Seismology Report No. 237, British Geological Survey
- 1111 Cara M, Cansi Y, Schlupp A, Arroucau P, Bethoux N, Beucler E, Bruno S (2015) SI-Hex: a  
 1112 new catalogue of instrumental seismicity for metropolitan France. *Bulletin de la Société*  
 1113 *Géologique de France* 188 (1-2):3-19
- 1114 Cauzzi C, Faccioli E, Vanini M, Bianchini M (2015) Updated predictive equations for  
 1115 broadband (0.01 to 10 s) horizontal response spectra and peak ground motions, based on a  
 1116 global dataset of digital acceleration records. *Bull Earthquake Eng* 13 (6):1587-1612
- 1117 Chadwick R A, Pharaoh A, Williamson J P, Musson R M W (1996) Seismotectonics of the  
 1118 UK. Technical report WA/96/3C, British Geological Survey
- 1119 Coatsworth A (2015) Forty years of earthquake engineering in the UK nuclear industry:  
 1120 Opportunities, failures and successes. SECED 2015 Conference: Earthquake Risk and  
 1121 Engineering towards a Resilient World, 9-10 July, Cambridge, UK
- 1122 Coppersmith K, Bommer J, Hanson K, Unruh J, Coppersmith R, Wolf L, Youngs B,  
 1123 Rodriguez-Marek A, Al Atik L, Toro G, Montaldo-Falero V (2014) Hanford sitewide  
 1124 probabilistic seismic hazard analysis. Technical Report PNNL-23361, Pacific Northwest  
 1125 National Laboratory, Richland, Washington 99352, USA
- 1126 Cornell C A (1968) Engineering seismic risk analysis. *Bull Seismol Soc Am* 58 (5):1583-  
 1127 1606
- 1128 Cotton F, Scherbaum F, Bommer J J, Bungum H (2006) Criteria for selecting and adjusting  
 1129 ground-motion models for specific target regions: application to central Europe and rock  
 1130 sites. *J Seismol* 10 (2):137-156
- 1131 Darendeli M B (2001) Development of a new family of normalized modulus reduction and  
 1132 material damping curves. PhD Thesis, Austin Texas: The University of Austin Texas, 393  
 1133 pgs
- 1134 Davis P D, Eldred P J L, Bennel J D, Hight D W, King M S (1996) Site investigation for  
 1135 seismically designed structures. Proceedings of Conference on Advances in Site Investigation  
 1136 Practice :715-726, Thomas Telford
- 1137 Delavaud E, Cotton F, Akkar S, Scherbaum F, Danciu L, Beauval C, Drouet S, Douglas J,  
 1138 Basili R, Sandikkaya M A, Segou M, Faccioli E, Theodoulidis N (2012) Toward a ground-  
 1139 motion logic tree for probabilistic seismic hazard assessment in Europe. *J Seismol* 16  
 1140 (3):451-473
- 1141 Douglas J (2014) Ground motion prediction equations 1964-2014. Accessed: September  
 1142 2014, <http://www.gmpe.org.uk>

- 1143 Douglas J (2018) Capturing geographically-varying uncertainty in earthquake ground motion  
1144 models or what we think we know may change. *Recent Advances in Earthquake Engineering*  
1145 in Europe, Ptilakis K (ed.), *Geotechnical, Geological and Earthquake Engineering* 46 :153-  
1146 181, Springer International Publishing AG, doi: 10.1007/978-3-319-75741-4\_6
- 1147 Douglas J, Cotton F, Di Alessandro C, Boore D M, Abrahamson N A, Akkar S (2012)  
1148 Compilation and critical review of GMPEs for the GEM-PEER global GMPEs project.  
1149 Lisbon, Portugal: Fifteenth World Conference on Earthquake Engineering :1-10
- 1150 Douglas J, Ulrich T, Bertil D, Rey J (2014) Comparison of seismic hazard uncertainties  
1151 among different studies. *Seismol Res Lett* 85 (5):977-985
- 1152 Edwards B, Rietbrock A, Bommer J J, Baptie B (2008) The acquisition of source, path, and  
1153 site effects from microearthquake recordings using Q tomography: Application to the United  
1154 Kingdom. *Bull Seismol Soc Am* 98:1915-1935
- 1155 EPRI (1994) The earthquake of stable continental regions – Volume 1: Assessment of large  
1156 earthquake potential. Report TR-10226-V1, Electric Power Research Institute, 370 pgs
- 1157 EPRI (2013) Seismic evaluation guidance: Screening, prioritization and implementation  
1158 details (SPID) for the resolution of Fukushima Near-Term Task Force recommendation 2.1.  
1159 Report 1025287, Electric Power Research Institute, Palo Alto, California, 220 pgs
- 1160 Franceseisme (2014) Catalogue BCSF-LDG: Informations techniques sur le contenu du  
1161 catalogue. Vers. 2014. Le Bureau Central Sismologique Français. French National Seismic  
1162 Monitory Network. Accessed 08 14, 2014. [http://www.franceseisme.fr/SIHex/SI-](http://www.franceseisme.fr/SIHex/SI-Hex_document-technique.pdf)  
1163 [Hex\\_document-technique.pdf](http://www.franceseisme.fr/SIHex/SI-Hex_document-technique.pdf)
- 1164 Grünthal G, Wahlström R, Stromeyer D (2009) The unified catalogue of earthquakes in  
1165 central, northern, and northwestern Europe (CENEC)—updated and expanded to the last  
1166 millennium. *J Seismol* 13:517-541
- 1167 Hara A, Kiyota Y (1977) Dynamic shear tests on soils for seismic analyses. *Proceedings of*  
1168 *9th ICSMFE* :257-260
- 1169 Hardwick A J (2008) New insights into the crustal structure of the England, Wales and Irish  
1170 Seas areas from local earthquake tomography and associated seismological studies. PhD  
1171 Thesis, University of Leicester
- 1172 IAEA (2010) Seismic hazards in site evaluation for nuclear installations. IAEA Safety  
1173 Standards Series No. SSG-9, Vienna: International Atomic Energy Agency
- 1174 Kaklamanos J, Bradley B A, Thomson R M, Baise L G (2013) Critical parameters affecting  
1175 bias and variability in site-response using KiK-net downhole data. *Bull Seismol Soc Am* 103  
1176 (3):1733-1749
- 1177 Kim Y-S (1992) Deformation characteristics of sedimentary soft rocks by triaxial  
1178 compression tests. Dr Engineering Thesis, University of Tokyo
- 1179 Kottke A R, Rathje E M (2013) Comparison of time series and random-vibration theory site-  
1180 response methods. *Bull Seismol Soc Am* 103 (3):2111-2127
- 1181 Kottke A R, Wang X, Rathje E M (2013) Technical manual for STRATA. Texas Austin:  
1182 Department of Civil, Architectural and Environmental Engineering, 103 pgs
- 1183 Kulkarni R B, Youngs R R, Coppersmith K J (1984) Assessment of confidence intervals for  
1184 results of seismic hazard analysis. *Proceedings of the Eighth World Conference on*  
1185 *Earthquake Engineering, Volume 1. San Francisco* :263-270

- 1186 Leonard M (2010) Earthquake fault scaling: Self-consistent relating of rupture length, width,  
1187 average displacement, and moment release. Bull Seismol Soc Am 100 (5A):1971-1988
- 1188 Lessi-Cheimariou A, Tromans I J, Rathje E, Robertson C (2018) Sensitivity of surface hazard  
1189 to different factors and site response analysis approaches: A case study for a soft rock site.  
1190 Bull Earthquake Eng, submitted
- 1191 McGuire R K (1976) FORTRAN computer program for seismic risk calculations. Open-File  
1192 Report 76, US Geological Survey, 67 pgs
- 1193 McGuire R K, Silva W J, Constantino C J (2001) Technical basis for revision of regulatory  
1194 guidance on design ground motions. NUREG/CR-6728, Washington D.C., Nuclear  
1195 Regulatory Commission, 143 pgs
- 1196 Meletti C, D'Amico V, Martinelli F (2010) Homogeneous determination of maximum  
1197 magnitude. Deliverable D3.3, Seismic Hazard Harmonization in Europe (SHARE), 23 pgs
- 1198 Musson R M W (1989) Seismicity of Cornwall and Devon. Technical report WL/89/11,  
1199 British Geological Survey
- 1200 Musson R M W (1994) A catalogue of British earthquakes. Technical report WL/89/11,  
1201 British Geological Survey
- 1202 Musson R M W (1996) Determination of parameters for historical British earthquakes.  
1203 Annali di Geofisica 39 (5):1041-1048
- 1204 Musson R M W (2005) Intensity attenuation in the UK. J Seismol 9:73-86
- 1205 Musson R M W (2007) British earthquakes. Proceedings of the Geologists' Association, Vol.  
1206 118:305-337
- 1207 Musson R M W (2008) The seismicity of the British Isles to 1600. Technical report  
1208 OR/08/049, British Geological Survey
- 1209 Musson, R M W (2012) PSHA validated by quasi observational means. Seismol Res Lett  
1210 83(1):130-134
- 1211 Musson R M W (2015) Bipartite earthquake magnitude-frequency distributions. Abstracts of  
1212 the IUGG/IASPEI 38th General Assembly. Prague
- 1213 Musson R M W, Sargeant S L (2007) Eurocode 8 seismic hazard zoning maps for the UK.  
1214 Technical report CR/07/125, British Geological Survey, 70 pgs
- 1215 Musson R M W, Chadwick R A, Pharaoh T C, Henni P H O, Wild B, Carney J N (2001)  
1216 Seismic hazard assessment for Wylfa. Technical report CR/01/253, British Geological Survey
- 1217 NAGRA (2004) Probabilistic seismic hazard analysis for Swiss nuclear power plant sites  
1218 (PEGASOS project). Site response characterisation (SP3). Final report PMT-SB-0006, Vol.  
1219 6, Nationale Genossenschaft für die Lagerung radioaktiver Abfälle, 367 pgs
- 1220 NE (1995) Hinkley Point 'C' power station, review of dynamic geotechnical properties.  
1221 Technical report HPC-IC-096521, Nuclear Electric, 566 pgs
- 1222 Nishi K, Kokusho T, Esashi Y (1983) Dynamic shear modulus and damping ratio of rocks for  
1223 a wide confining pressure range. Proceedings of the 5th Congress ISRM. Melbourne :223-  
1224 226
- 1225 Ordaz M, Martinelli F, Aguilar A, Arboleda J, Meletti C, D'Amico V (2015) Crisis2015 Ver.  
1226 1.0: Program for computing seismic hazard. Instituto de Ingeniería, UNAM

- 1227 Ottemöller L, Sargeant S (2010) Ground-motion difference between two moderate-size  
1228 intraplate earthquakes in the United Kingdom. *Bull Seismol Soc Am* 100 (4):1823-1829
- 1229 Ottemöller L, Baptie B, Smith N J P (2009) Source parameters for the 28 April 2007 Mw 4.0  
1230 earthquake in Folkestone, United Kingdom. *Bull Seismol Soc Am* 99 (3):1853-1867
- 1231 Pagani M, Monelli D, Weatherill G, Danciu L, Crowley H, Silva V, Henshaw P, et al. (2014)  
1232 OpenQuake Engine: An open hazard (and Risk) software for the Global Earthquake Model.  
1233 *Seismol Res Lett* 85 (3):692-702
- 1234 Pearson, E S, Tukey J W (1965) Approximate Means and Standard Deviations Based on  
1235 Distances Between Percentage Points of Frequency Curves. *Biometrika* 52 (3-4): 533-546
- 1236 Principia Mechanica Ltd (1982) *British Earthquakes*. Cambridge, UK, Principia Mechanica  
1237 Ltd
- 1238 Renault P (2014) Approach and challenges for the seismic hazard assessment of nuclear  
1239 power plants: the Swiss experience. *Bolletino di Geofisica Teorica ed Applicata* 55 (1):149-  
1240 164
- 1241 Renault P (2015) PEGASOS Refinement Project: A refined seismic hazard assessment for  
1242 Swiss nuclear power plants. 14 D-A-CH Conference - Earthquakes and existing buildings,  
1243 Zurich, 8 pgs. (In German)
- 1244 Rietbrock A, Strasser F, Edwards B (2013) A stochastic earthquake ground-motion prediction  
1245 model for the United Kingdom. *Bull Seismol Soc Am* 103 (1):57-77
- 1246 Rodriguez-Marek A, Rathje E M, Bommer J J, Scherbaum F, Stafford P J (2014) Application  
1247 of single-station sigma and site-response characterisation in a probabilistic seismic hazard  
1248 analysis for a new nuclear site. *Bull Seismol Soc Am* 104 (4):1601-1619
- 1249 Rodriguez-Marek A, Cotton F, Abrahamson N A, Akkar S, Al Atik L, Edwards B, Montalva  
1250 G A, Dawood H M (2013) A model for single-station standard deviation using data from  
1251 various tectonic regions. *Bull Seismol Soc Am* 103 (6):3149-3163
- 1252 Sargeant S L, Ottemöller L (2009) Lg wave attenuation in Britain. *Geophys J Int* 179:1593-  
1253 1606
- 1254 Scherbaum F, Kuehn N (2011) Logic tree branch weights and probabilities: Summing up to  
1255 one is not enough. *Earthq Spectra* 27 (4):1237-1251
- 1256 Scherbaum F, Delavaud E, Riggelsen C (2009) Model selection in seismic hazard analysis:  
1257 an information-theoretic perspective. *Bull Seismol Soc Am* 99 (6):3234-3247
- 1258 Scherbaum F, Cotton F, Smit P (2004) On the use of response spectral reference data for the  
1259 selection and ranking of ground motion models for seismic hazard analysis in regions of  
1260 moderate seismicity: The case of rock motion. *Bull Seismol Soc Am* 94 (6):2164-2185
- 1261 Scherbaum F, Kuehn N M, Ohrnberger M, Koehler A (2010) Exploring the proximity of  
1262 ground-motion models using high-dimensional visualization techniques. *Earthq Spectra* 26  
1263 (4):1117-1138
- 1264 SHWP (1987) Report on seismic hazard assessment. Hinkley Point, Volume 2A: Seismic  
1265 Hazard Working Party, Central Electricity Generating Board, 416 pgs
- 1266 SHWP (1989) Volume 2A Annex, Report on microseismic network results, January 1987 -  
1267 August 1989. Seismic Hazard Working Party, Central Electricity Generating Board, 95 pgs
- 1268 Soil Mechanics Ltd (1982) Reassessment of UK seismicity data. Bracknell, UK, Soil  
1269 Mechanics Ltd.

1270 Stepp J C, Wong I, Whitney J, Quittmeyer R, Abrahamson N, Toro G, Youngs R.,  
1271 Coppersmith K, Savy J, Sullivan T, Yucca Mountain PSHA Project members (2001)  
1272 Probabilistic seismic hazard analyses for ground motions and fault displacement at Yucca  
1273 Mountain, Nevada. *Earthq Spectra* 17 (1):113-151

1274 Stewart J P, Afshari Y M A (2014) Guidelines for performing hazard-consistent one-  
1275 dimensional ground response analysis for ground motion prediction. 2014/16, October 2014,  
1276 California: Pacific Earthquake Engineering Research Center, 152 pgs

1277 Stewart J P, Douglas J, Javanbarg M, Bozorgnia Y, Abrahamson N A, Boore D M, Campbell  
1278 K W, Delavaud E, Erdik M, Stafford P J (2015) Selection of ground motion prediction  
1279 equations for the Global Earthquake Model. *Earthq Spectra* 31 (1):19-45

1280 Toro G R (1995) Probabilistic models of site velocity profiles for generic and site-specific  
1281 validation of the stochastic ground motion model. New York, Brookhaven National  
1282 Laboratory

1283 USNRC (2007) A performance-based approach to define the site-specific earthquake ground  
1284 motion. Regulatory Guide 1.208, U.S. Nuclear Regulatory Commission

1285 Van Houtte C, Drouet S, Cotton F (2011) Analysis of the origins of kappa to compute hard  
1286 rock to rock adjustment factors for GMPEs. *Bull Seismol Soc Am* 101 (6):2926-2941

1287 Whittaker A, Brereton N R, Evans C J, Long R E (1989) Seismotectonics and crustal stress in  
1288 Great Britain. *Earthquakes at North-Atlantic passive margins: Neotectonics and postglacial  
1289 rebound* :663-664, edited by S. Gregersen and P. W. Basham, Kluwer Academic Publishers

1290 Woessner J, Laurentiu D, Giardini D, Crowley H, Cotton F, Grünthal G, Valensise G,  
1291 Arvidsson R, Basili R, Demircioglu M B, Hiemer S, Meleti C, Musson R M W, Rovida A N,  
1292 Sesetyan K, Stucchi M, The SHARE Consortium (2015) The 2013 European seismicity  
1293 hazard model: key components and results. *Earthquake Engineering* 13 (12):3553-3596

1294